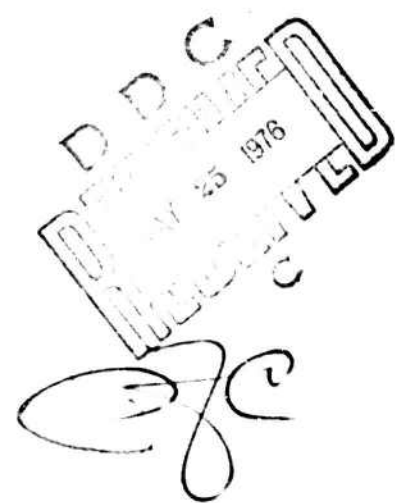


AD A024744



Report DARCOM-ITC-02-08-76-006

FEASIBILITY STUDY OF PERFORMING SYSTEM CALIBRATION IN AN OPERATE MODE

Robert Joseph Gorak  
Maintenance Effectiveness Graduate Program  
DARCOM Intern Training Center  
Red River Army Depot  
Texarkana, Texas 75501

April 1976



Final Report

APPROVED FOR PUBLIC RELEASE: DISTRIBUTION UNLIMITED

Prepared for

MAINTENANCE EFFECTIVENESS GRADUATE PROGRAM  
AND TEXAS A&M UNIVERSITY GRADUATE CENTER  
DARCOM Intern Training Center  
Red River Army Depot  
Texarkana, Texas 75501

REPORT DOCUMENTATION PAGE		READ INSTRUCTIONS BEFORE COMPLETING FORM
1. REPORT NUMBER 14) DARCOM-ITC-02-08-76-006	2. GOVT ACCESSION NO.	3. RECIPIENT'S CATALOG NUMBER
4. TITLE (and Subtitle) FEASIBILITY STUDY OF PERFORMING SYSTEM CALIBRATION IN AN OPERATE MODE.		5. TYPE OF REPORT & PERIOD COVERED 9) Final Sept.
6. PERFORMING ORG. REPORT NUMBER		
7. AUTHOR(s) 10) Robert Joseph Gorak	8. CONTRACT OR GRANT NUMBER(s)	
9. PERFORMING ORGANIZATION NAME AND ADDRESS Maintenance Effectiveness Graduate Engineering Program, DARCOM Intern Training Center, Red River Army Depot, Texarkana, Texas 75501		10. PROGRAM ELEMENT, PROJECT, TASK AREA & WORK UNIT NUMBERS 12) 95P.
11. CONTROLLING OFFICE NAME AND ADDRESS Maintenance Effectiveness Graduate Engineering Program and Texas A&M University Graduate Center, DARCOM Intern Training Center		12. REPORT DATE 11) Apr 1976
14. MONITORING AGENCY NAME & ADDRESS (if different from Controlling Office)		13. NUMBER OF PAGES 84
		15. SECURITY CLASS. (of this report)
		15a. DECLASSIFICATION/DOWNGRADING SCHEDULE
16. DISTRIBUTION STATEMENT (of this Report)  APPROVED FOR PUBLIC RELEASE: DISTRIBUTION UNLIMITED		
17. DISTRIBUTION STATEMENT (of the abstract entered in Block 20, if different from Report)		
18. SUPPLEMENTARY NOTES  Research performed by Robert J. Gorak under the supervision of Dr. John M. CoVan, Assistant Professor, Industrial Engineering Department, Texas A&M University.		
19. KEY WORDS (Continue on reverse side if necessary and identify by block number)  Calibration, Gyroscopes, Inertial Navigation, Perturbation.		
20. ABSTRACT (Continue on reverse side if necessary and identify by block number)  The availability of a system can be upgraded if the usual downtime allocated for performing calibration tasks is reduced or eliminated. The objective of this paper is to study the feasibility of performing the calibration of system parameters while the system is in an operate mode. To this end, a calibration technique exhibiting this feature was developed and studied for a marine inertial navigation system. The errors introduced by the calibration technique were examined and problematic areas were outlined. → OVF		

*Copy*

SECURITY CLASSIFICATION OF THIS PAGE(When Data Entered)

Although the report is directed specifically towards the calibration of certain parameters of a particular system, the ideas and concepts presented in the development of the report's calibration technique should be applicable to other systems for the elimination of all or some of their calibration downtime. The formulation of a similar type of calibration procedure is especially desirable for systems whose unavailability at a time of critical need could result in a catastrophic loss of men, material and tactical advantage.

↑



9

SECURITY CLASSIFICATION OF THIS PAGE(When Data Entered)

## FOREWORD

The research discussed in this report was accomplished as part of the Maintenance Effectiveness Graduate Program conducted jointly by the DARCOM Intern Training Center and Texas A&M University. As such, the ideas, concepts and results herein presented are those of the author and do not necessarily reflect approval or acceptance by the Army.

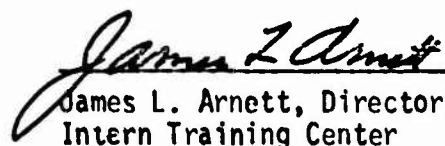
This report has been reviewed and is approved for release. For further information on this project contact Dr. Ronald C. Higgins, Chief of Maintenance Effectiveness, Red River Army Depot, Texarkana, Texas.

Approved:



Dr. Ronald C. Higgins, Chief  
Maintenance Effectiveness Engineering

For the Commander



James L. Arnett, Director  
Intern Training Center

## ABSTRACT

Research Performed by Robert J. Gorak  
Under the Supervision of Dr. John M. CoVan

The availability of a system can be upgraded if the usual downtime allocated for performing calibration tasks is reduced or eliminated. The objective of this paper is to study the feasibility of performing the calibration of system parameters while the system is in an operate mode. To this end, a calibration technique exhibiting this feature was developed and studied for a marine inertial navigation system. The errors introduced by the calibration technique were examined and problematic areas were outlined.

Although the report is directed specifically towards the calibration of certain parameters of a particular system, the ideas and concepts presented in the development of the report's calibration technique should be applicable to other systems for the elimination of all or some of their calibration downtime. The formulation of a similar type of calibration procedure is especially desirable for systems whose unavailability at a time of critical need could result in a catastrophic loss of men, material and tactical advantage.

## ACKNOWLEDGMENTS

The author wishes to express his appreciation to Dr. John M. CoVan, Assistant Professor of Industrial Engineering, under Texas A&M University, for his guidance and assistance throughout the preparation of this paper.

During the course of this work, the author was employed by the Department of the Army as a career intern in the AMC Maintainability Engineering Graduate Program. He is grateful to the United States Army Materiel Command for the opportunity to participate in this program.

The ideas, concepts and results herein presented are those of the author, and do not necessarily reflect the approval or acceptance of the Department of the Army.

## TABLE OF CONTENTS

Chapter		Page
I	INTRODUCTION . . . . .	1
	Statement of Problem. . . . .	1
	Method of Approach. . . . .	2
	Calibration Technique Example . . . . .	3
	Chapter Summary . . . . .	9
II	BACKGROUND . . . . .	11
	Gyro Calibration. . . . .	11
	Fourth Gyro Utilization. . . . .	11
	Inertial Platform Positioning. . . . .	12
	Continuous Platform Rotation . . . . .	12
	Relationship of Report's Calibration Technique to Existing Techniques. . . . .	14
	Integration of Report's Calibration Technique with Existing Techniques. . . . .	15
III	MARINE INERTIAL NAVIGATION SYSTEM. . . . .	17
	General Description . . . . .	17
	Major Components. . . . .	18
	Accelerometers . . . . .	18
	Gyroscopes . . . . .	20
	A Damped Inertial Navigation System . . . . .	22
	Platform Stabilization . . . . .	22
	System Function. . . . .	25
	Error Model. . . . .	25
	System Disturbances. . . . .	28
	Navigation Errors. . . . .	28
	Need for Calibration. . . . .	29
IV	CALIBRATION TECHNIQUE. . . . .	31
	Source of Perturbation. . . . .	33
	Generation of Perturbation Signal . . . . .	34
	Development of Model. . . . .	39
	Perturbation Effects . . . . .	39
	Observation Errors . . . . .	41
	Outside Disturbances . . . . .	42
	Confidence Limits and Statistical Tests . . . . .	45
	Additional Estimate Efficiency. . . . .	47
	Calibration Technique Summary . . . . .	49
	Discussion of Calibration Technique . . . . .	51

Chapter		Page
V	ERROR ANALYSIS . . . . .	54
	Uncalibrated Parameter Error. . . . .	54
	Calibration Induced Error . . . . .	56
	Error in Calibration Results. . . . .	58
VI	CONCLUSIONS. . . . .	64
	REFERENCES . . . . .	66
	APPENDIX A . . . . .	68
	APPENDIX B . . . . .	78

## LIST OF FIGURES

Figure		Page
1.1	FUNCTIONAL DIAGRAM OF EXEMPLARY AMPLIFICATION SYSTEM . . . . .	4
1.2	SQUARE WAVE PERTURBATION SIGNAL . . . . .	5
1.3	FUNCTIONAL DIAGRAM OF THE IMPLEMENTATION OF THE EXEMPLARY CALIBRATION TECHNIQUE . . . . .	8
3.1	TORQUED-PENDULUM ACCELEROMETER. . . . .	19
3.2	SINGLE-DEGREE-OF-FREEDOM INTEGRATING RATE GYRO. . . . .	21
3.3	THREE GIMBAL CONFIGURATION. . . . .	24
3.4	FUNCTIONAL DIAGRAM OF MARINE INERTIAL NAVIGATION SYSTEM . . . . .	26
3.5	ERROR MODEL FOR MARINE INERTIAL NAVIGATION SYSTEM . . . . .	27
4.1	GYRO INPUT AXIS MISALIGNMENT ANGLES . . . . .	32
4.2	EXCURSION ANGLE . . . . .	36
4.3	THE PERTURBATION SIGNAL (X-AXIS ACCELERATION). . . . .	37
4.4	X-VELOCITY LOOP ERROR MODEL . . . . .	38
4.5	VELOCITY OUTPUT CONTAINING MISALIGNMENT ANGLE INFORMATION . . . . .	40
4.6	TYPICAL VELOCITY OUTPUT DATA FOR ESTIMATION MODEL . . . . .	44
4.7	STUDENT-T DISTRIBUTION (3 DEGREES OF FREEDOM) . . . . .	48
5.1	ACCELEROMETER AND GYRO DRIFT RATE ERRORS. . . . .	57
5.2	CROSS AXIS GYRO DRIFT RATE ERRORS . . . . .	59
A.1	REFERENCE VELOCITY RESOLUTION . . . . .	69
A.2	VELOCITY ERROR MODEL. . . . .	71
A.3	ACCELERATION ERROR SIGNAL . . . . .	74

## LIST OF TABLES

Table		Page
5.1	NAVIGATION ERRORS - UNCALIBRATED PARAMETER . . . . .	55
5.2	NAVIGATION ERRORS - UNCALIBRATED PARAMETER OF ONE ARC MINUTE AT A LATITUDE OF 45 DEGREES . . . . .	55
5.3	NAVIGATION ERRORS - INDUCED ACCELERATION DISTURBANCE . . . . .	60
5.4	NAVIGATION ERRORS - GYRO DRIFT RATE DISTURBANCE . . . . .	60
5.5	NAVIGATION ERRORS - CROSS-AXIS GYRO DRIFT RATE (INDUCED PLATFORM ROTATION) . . . . .	61
5.6	NAVIGATION ERRORS - CROSS-AXIS GYRO DRIFT RATE (EARTH ROTATIONAL RATE) . . . . .	61
5.7	TOTAL NAVIGATION ERRORS - CALIBRATION TECHNIQUE. . . . .	62
5.8	TOTAL NAVIGATION ERRORS - CALIBRATION TECHNIQUE ( $\theta = 1$ ARC MINUTE; $L = 45$ DEGREES) . . . . .	62

## CHAPTER I

### INTRODUCTION

Calibration in many systems is needed during a corrective maintenance action when a major system component is replaced. In other systems, calibration is done on a periodic basis for preventive maintenance purposes to insure that system accuracy is maintained. In both cases this normally requires that the system be kept or brought down into a non-operate mode for the duration of the calibration procedure. If the required downtime for calibration is significant with respect to the mean operational time between maintenances, the operational availability of the system is reduced consequently. However, many systems such as the Polaris marine inertial navigation system require the maximum attainable availability during a mission. The availability of a system can be upgraded if the downtime required for calibration is eliminated by a technique which performs calibration swiftly and accurately while the system is in an operate mode.

It is the objective of this report to study a formulation of such a technique for a precision marine inertial navigation system. This system was chosen not only to investigate the feasibility of performing system calibration in an operate mode on a practical system but also to study the applicability of the technique to a system whose mode of operation requires the need for a profound investigation of the calibration errors and of the system errors from such a calibration technique.

#### Statement of Problem

The principle purpose of an inertial navigation system is to provide,

independent of any external sources of reference, positional data for a vehicle. This is accomplished with the employment of three accelerometers and three single degree-of-freedom gyros along with their associated electronics. The three accelerometers are aligned such that their sensitive axes are mutually perpendicular to each other forming a three axes coordinate system. Each gyro sensitive axis is then aligned along one of the three axes of the coordinate system. Any initial misalignment of the gyros with respect to this coordinate system will produce an undetectable error when the system is operational and degrade system accuracy. A calibration scheme is therefore necessary to compute these misalignments.

#### Method of Approach

Simply, the technique proposed in this report requires the inducement of a signal of prescribed frequency and amplitude into the system (a system perturbation signal) and the determination of the gyro misalignments by filtering the outputs of various system components.

There are two major sources of error, when the aforesaid technique is used. One is the error produced by the initial gyro misalignments over the time in which the calibration scheme is calculating them. The second is the error introduced into the system by the proposed calibration technique of perturbation. Both of these errors can be minimized by minimizing the time required by the calibration technique. It is proposed that this minimization can be accomplished by a proper selection of the perturbation signal period and amplitude. Bearing in mind the dynamic limitations of the system, a relatively high frequency can be so chosen to permit an estimate of the gyro misalignments in a short period of time. These results at the option of the responsible engineer can then be systematically

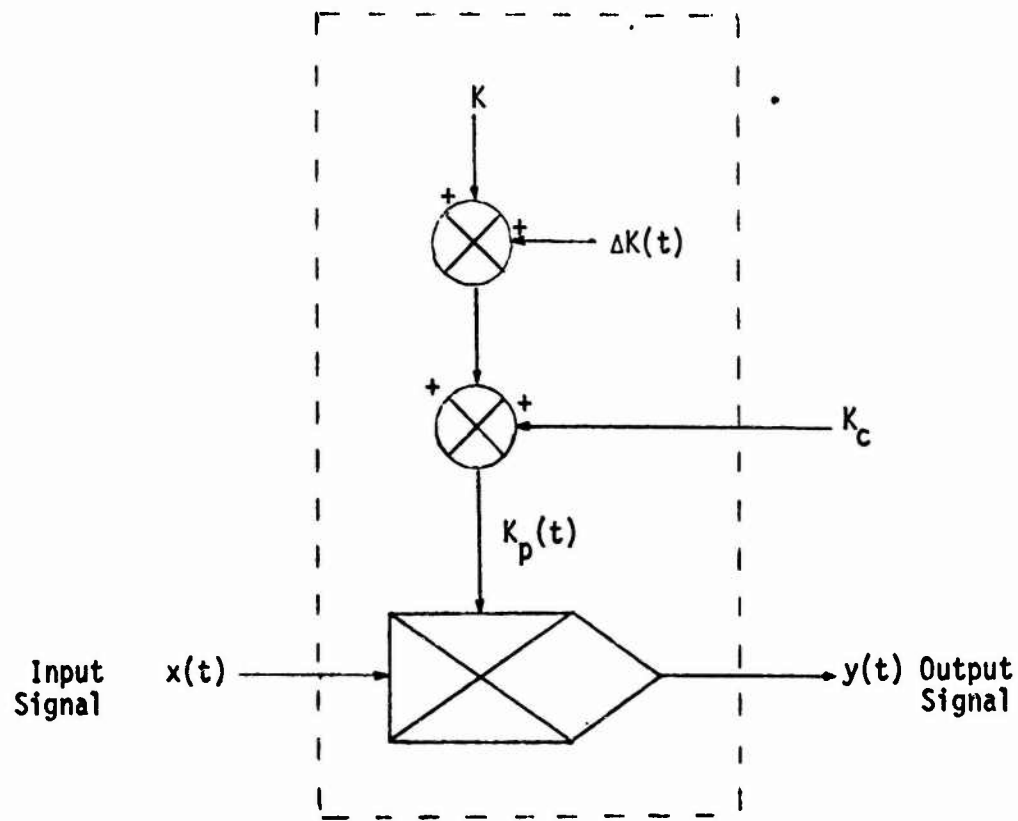
applied to the system every signal period thus reducing the errors due to possibly large initial gyro misalignments. The short perturbation signal period also allows for the collection of several sample estimates thus increasing the precision of the calibration. A median must be reached, however, between the total number of estimates obtained and the amount of error introduced by the perturbation to the system.

#### Calibration Technique Example

Since the purpose of this report is to investigate the feasibility of performing system calibration in an operate mode, it is vital that the reader have a clear understanding of the basic processes involved in this calibration technique. To this end, a simple example is now presented and a calibration technique is devised. In addition, the introduction of this example affords the author the opportunity to preview the various problematic areas of his calibration technique to be presented and discussed in the latter chapters of this report.

The example employs a system whose function is that of amplifying an input signal. The amplifier's gain constant,  $K$ , is an unobservable, integral part of the system and the sole parameter of the system. It is assumed that this system parameter does not remain constant over time but changes in discrete steps,  $\Delta K(t)$ , over extended periods of time. It is also assumed that the system has a means of correcting for these changes once they are known. Thus, the function of calibration is to determine the present value,  $K_p(t)$ , of this system parameter and to correct it by inserting a correction factor,  $K_c$ , to the system. A functional diagram of this system is presented in Figure 1.1.

A possible calibration procedure would be to introduce a known



FUNCTIONAL DIAGRAM OF  
EXEMPLARY AMPLIFICATION SYSTEM

FIGURE 1.1

constant input to the system and observe the output. The present value of the system parameter would equal the output divided by the input. However, this procedure requires that the system be placed into a non-operate mode for some period of time. This downtime may be substantial if the total downtime is considered. The total downtime, in general, consists of the time to:

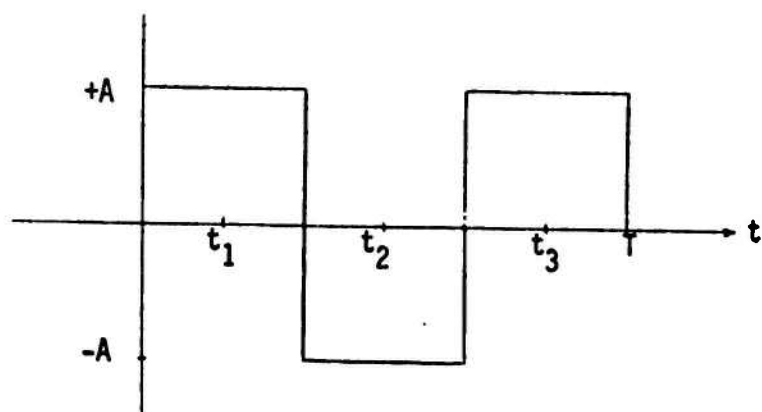
- 1) remove the system from an operate mode,
- 2) place the system in a calibrate mode,
- 3) calibrate the system, and
- 4) replace the system in an operate mode.

This total downtime can be eliminated by using a technique whereby calibration is performed while the system is operating. For this example, such a technique can be formulated provided general knowledge of the input signal is available. To simplify the technique for the example, it is assumed that the input signal which is of arbitrary form can be described accurately by a linear equation (Eq. 1.1) over a short period of time, T.

$$x(t) = a + b t \quad 0 \leq t \leq T \quad (1.1)$$

Under the above assumption and the additional assumption that the system parameter remains constant over the time of calibration, the calibration of the system parameter can be accomplished while the system is operating by:

- 1) the superposition, on the input signal, of a square wave signal (the perturbation signal) of amplitude, A, and the period,  $2T/3$ , for a time period equal to T (Fig. 1.2),
- 2) the observation of the output at the times  $t_1$ ,  $t_2$  and  $t_3$  shown in Figure 1.2, and
- 3) the calculation of the present value of the system parameter,



SQUARE WAVE  
PERTURBATION SIGNAL

FIGURE 1.2

using the information obtained in step (2), by Equation 1.2 and the calculation of the correction factor by Equation 1.3.

$$K_p = (y(t_1) - 2y(t_2) + y(t_3))/4A \quad (1.2)$$

$$K_c = K - K_p \quad (1.3)$$

Following the procedure as outlined above, the outputs at times  $t_1$ ,  $t_2$  and  $t_3$  are described by Equations 1.4.

$$\begin{aligned} y(t_1) &= K(a + bt_1) + \Delta K(a + bt_1) + A(K + \Delta K) \\ y(t_2) &= K(a + bt_2) + \Delta K(a + bt_2) - A(K + \Delta K) \\ y(t_3) &= K(a + bt_3) + \Delta K(a + bt_3) + A(K + \Delta K) \end{aligned} \quad (1.4)$$

In substituting the known relationships between the times  $t_2$  and  $t_3$  and the time  $t_1$

$$t_2 = 3t_1$$

$$t_3 = 5t_1$$

into Equation 1.4, the present value of the system parameter and the required correction factor are obtained as follows:

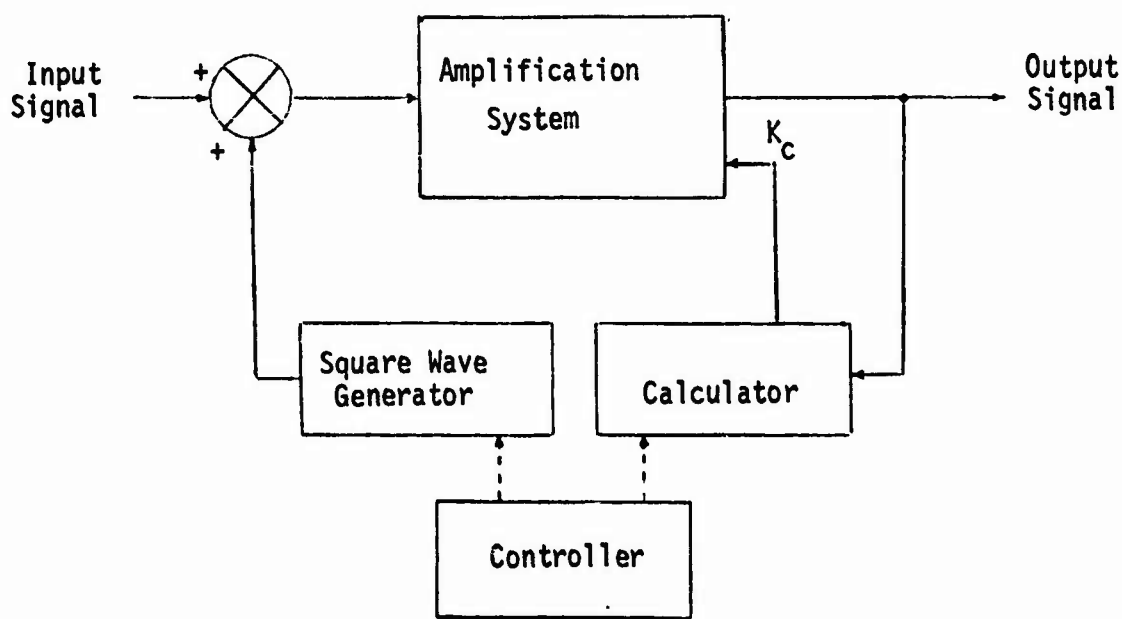
$$K_p = \left[ \begin{array}{l} + (a + bt_1)(K + \Delta K) + A(K + \Delta K) \\ -2(a + 3bt_1)(K + \Delta K) + 2A(K + \Delta K) \\ + (a + 5bt_1)(K + \Delta K) + A(K + \Delta K) \end{array} \right] + 4A$$

$$K_p = K + \Delta K$$

$$K_c = K - K_p = -\Delta K$$

Thus, insertion of this correction factor ( $-\Delta K$ ) into the system (Fig. 1.1) provides the desired result, namely that of proper system operation. The calibration technique for this example is functionally presented in Figure 1.3.

This example presents the two errors existing in the system during calibration as referred to earlier in this chapter. The second terms in Equations 1.4 represent the error produced by the system parameter error.



FUNCTIONAL DIAGRAM  
OF THE  
IMPLEMENTATION OF THE EXEMPLARY  
CALIBRATION TECHNIQUE

FIGURE 1.3

The third terms of Equations 1.4 represent the error due to the perturbation signal. These errors must be investigated and minimized to the extent that they fall within the particular system's error specifications.

In addition to these errors, the following general problematic areas arise when this report's calibration technique is employed.

- \* Is additional hardware needed? If so, can it be justified?
- \* How accurate can the input signal be described by the proposed model? Should a different model for the input signal be employed?
- \* Is it physically possible to observe the output signal at the times required by the calibration technique?
- \* Will the dynamics of the system prevent the insertion of the perturbation signal?
- \* How often does the system parameter which is being calibrated change?
- \* In what way will measurement errors affect the calibration results?
- \* At what magnitude of the perturbation signal amplitude will system operation deteriorate?

These problematic areas will be discussed in the following chapters with regard to this report's proposed calibration technique for a marine inertial navigation system.

#### Chapter Summary

Chapter II explores existing calibration techniques used to calibrate the gyro parameters of a marine inertial navigation system. Discussion is focused on the Navigate Theta-D technique and the SEASCAN technique and their relationship to this report's calibration technique.

The marine inertial navigation system is examined in Chapter III.

Its function is defined and its major components are investigated. Its overall operation is described and an error model for the system is presented. The need for calibration is also explored.

In Chapter IV, the proposed perturbation technique for the calibration of certain gyro misalignment angles in an operate mode is presented and a number of problematic areas outlined previously in this chapter are discussed. The source of the perturbation and the generation of the perturbation signal is presented. The method for determining an estimate of the gyro misalignment angle is developed considering observation errors and outside disturbances. Confidence limits are evolved under certain assumptions for the estimator and an example of a possible statistical test for parameter confidence is developed. A procedure to obtain a more efficient estimator is also suggested.

Chapter V discusses the errors present while calibration is being performed. Discussion is centered on the effect of gyro misalignments during calibration and the errors introduced by perturbation.

Chapter VI summarizes the author's opinion of the report's technique of calibrating system parameters and presents conclusions and recommendations for future analyses.

## CHAPTER II

### BACKGROUND

This chapter presents various techniques used to calibrate gyro parameters of a marine inertial navigation system. These parameters are the gyro drift bias, the gyro scale factor and the misalignment angles of the gyro input axis. A discussion of these parameters is deferred to Chapter III where a full treatment of the marine inertial navigation system and its components is presented. These gyro calibration techniques are presented as a background for this report's calibration scheme.

It should be noted that this report's calibration technique draws its basic concepts from these existing techniques and that the development of the technique via modifications to these existing schemes was promoted by the author's desire to maximize system operational availability by reducing the downtime needed for calibration.

#### Gyro Calibration

From the author's literature survey, the techniques for calibration of gyro parameters employ the following three approaches:

- (1) utilization of a fourth gyro,
- (2) inertial platform positioning, and
- (3) continuous inertial platform rotation.

#### Fourth Gyro Utilization

The researched technique using the first approach calibrates the gyro drift bias and gyro scale factor parameters for the three gyros of the marine inertial navigation system. Calibration is accomplished by aligning the axes of the fourth gyro with the axes of the gyro being

calibrated and measuring the effect on the fourth gyro of the application of a known disturbance to the gyro to which it is aligned. References (11), (12) and (17) provide a detailed description of this calibration technique. This type of calibration can be performed while the vehicle containing the inertial navigation system is at sea, but the system is unable to perform its navigation function while the calibration is in process. Calibration time is approximately two hours.

#### Inertial Platform Positioning

The techniques employing the second approach usually require a lengthy amount of time. Reference (8) describes such a technique for a marine inertial navigation system which has a fourth gyro. The technique known as the Coarse Align Theta D Calibration Technique calibrates the gyro scale factor and gyro input axis misalignment parameters for all the gyros. Calibration is performed by positioning the inertial platform, on which the three gyros are mounted, to various orientations. At each orientation, information is obtained from the four gyros and is used to calculate the gyro parameters. The technique requires approximately 28 hours to perform and can only be used dockside in a non-navigate mode.

#### Continuous Platform Rotation

The techniques using the third approach are based on the principle that rotation of the inertial platform while in the navigate mode introduces navigation errors which are known functions of the various uncalibrated gyro parameters. Reference (8) describes the Navigate Theta D Gyro Calibration Technique. This technique calibrates the gyro scale factor and gyro input axis misalignment parameters for the gyros of the marine inertial navigation system. During calibration, the inertial

platform is continuously rotated about its vertical axis at a rate of 25 degrees per hour until it has completed one full revolution. This rotation is accomplished by the application of a constant torque to the vertical gyro via the navigation system computer. As the platform rotates, the position of the vehicle as determined by the navigation system under calibration is obtained at specific times and compared to the position as determined by a simultaneously operating marine inertial navigation system or by some other reference source of position (such as the stars or orbiting satellites). The resulting difference in the determined vehicle positions is used by a computer program in solving a set of matrix equations using least squares estimations to yield the gyro parameters of concern. The calibration technique takes approximately 14.4 hours and can be performed while the vehicle is at sea. During the calibration the inertial navigation system is operated in a "Navigate Theta D" mode which is a pseudo-operational mode; that is, although during calibration the system is in a navigation mode, the navigation data secured from the system under calibration is not used due to the possibly large navigation errors introduced by the calibration technique. For further details on these errors, the reader is referred to Reference (10).

A second technique employing platform rotation is the SEASCAN (Simultaneous East Angular Sensor Calibration and Navigation) technique described by Reference (6). This technique calibrates the east gyro drift bias parameter of a marine inertial navigation system while the inertial navigation function continues uninterrupted. Calibration is accomplished by rotating the inertial platform at a fixed rate,  $r$ , or 60 degrees per hour via the vertical gyro torquer. The inertial platform is rotated 180 degrees at the rate  $r$ , then back 180 degrees at the rate

-r. During platform rotation, the east velocity output is continuously monitored and differenced with the east velocity as determined by an external velocity reference such as the electro-magnetic log or by another simultaneously operating marine inertial navigation system. The east gyro drift bias parameter is determined from this differenced velocity. The time for calibration is six hours. Details concerning the navigation errors present while calibration is being performed were not presented in the reference.

The author will mention two other calibration techniques which employ continuous inertial platform rotation. However, since they are classified, the author was unable to obtain detailed information concerning their implementation. Both calibration techniques were developed by Sperry Systems Management located at Lake Success, New York and are performed on a marine inertial navigation system which employs a fourth gyro. The first technique calibrates the level gyro input axis misalignment about a horizontal axis (either X or Y), the vertical gyro scale factor and other system parameters by rotating the inertial platform about the heading axis in a prescribed manner. Calibration time is approximately 6 hours. The second technique calibrates the level gyro input axis misalignment about the vertical axis and a fourth gyro parameter by rotating the inertial platform about the pitch axis in a prescribed manner. Calibration time is approximately 1 to 1.5 hours.

#### Relationship of Report's Calibration Technique to Existing Techniques

The technique formulated in this report was developed from the schemes presented in this chapter. In particular, the technique employs the rotation of the inertial platform via torques applied to the vertical

gyro in determining the gyro parameters of interest. In addition to bound the navigation errors resulting from the uncalibrated gyro parameters, the technique employs the procedure of rotating the platform a few degrees from its normal operating position while in a navigation mode.

#### Integration of Report's Calibration Technique with Existing Techniques

The system parameters of interest in this report are the X-gyro input axis misalignment about the Y-axis, and the Y-gyro input axis misalignment about the X-axis. The underlying motive for the formulation of a calibration technique for these parameters was the maximization of the system operational availability by the reduction of the time needed for calibration. The time required for calibration of these parameters using this report's calibration technique is approximately 25 minutes which is a 12 : 1 improvement over the minimum time required by the existing techniques.

However, in the event of a level gyro failure during a mission, full calibration of the replacement gyro is needed; namely, the calibration of the gyro drift bias, the gyro scale factor and the two gyro input axis misalignment parameters. Calibration of the gyro drift bias and the gyro scale factor parameters may be accomplished by a modification of the technique described by Reference (17). As noted earlier the calibration of these parameters for all the gyros requires approximately 2 hours. By restricting calibration to one gyro the author believes that the two gyro parameters could be calibrated in approximately 40 to 60 minutes. The calibration of the gyro input axis misalignment about the vertical axis may be obtained via the earlier mentioned technique developed by Sperry Systems Management. The time required for calibration is 60 to

90 minutes. Finally, the calibration of the gyro input axis misalignment about the horizontal may be performed via this report's calibration technique requiring approximately 25 minutes. This full gyro calibration procedure results in a total time of from 2 to 3 hours which is a 3 : 1 improvement over the best procedure resulting from a combination of the existing techniques.

Before presenting this report's calibration technique, Chapter III will orient the reader with the operation of a marine inertial navigation system.

## CHAPTER III

### THE MARINE INERTIAL NAVIGATION SYSTEM

The overall operation of a marine inertial navigation system is presented in this chapter. Discussion is focused on the inertial navigation system's major components and their role in navigating. The discussion of the navigation system will be general; however, the reader may refer to References (4), (18) and (19) for a more detailed description of the system. A particular navigation system is selected and an error model for the system is presented. This selected system is employed in the formulation of this report's calibration technique for a particular system parameter. The need for a technique to calibrate this parameter is also explored.

#### General Description

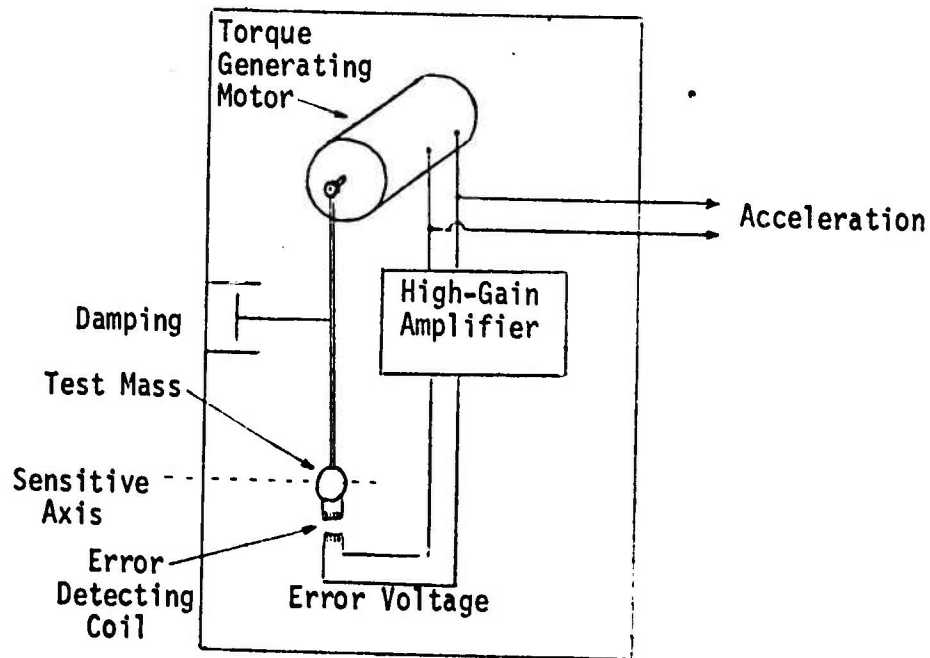
Inertial navigation is concerned with establishing the position, attitude and velocity of a vehicle, through measurements made by inertial sensors. In moving from one point to another, the vehicle executes a combination of linear and angular motions. The two sensors which are utilized to measure these motions are the accelerometer and gyroscope, respectively. These two devices are the only measuring instruments in a pure inertial navigator. The remainder of the system is essentially computational, converting the measurements into position, velocity and attitude in the desired reference frame. The marine inertial navigation system is a self-contained system. It doesn't depend on outside sources of information to perform its navigation function and

thusly free from enemy interference, the necessity for cooperative ground stations or the uncertainties of the weather.

### Major Components

#### Accelerometers

Craft position is determined from a double integration of directly measured acceleration by measuring reaction forces sensed entirely within the craft. This property of acceleration, that is, its direct proportionality to reaction forces as expressed by Newton's Second Law, is the fundamental principle of the accelerometer. The essential element of an accelerometer is the test mass or inertial element. The force required to hold the test mass stationary relative to an accelerating craft is used as a measure of the acceleration of the craft in which the accelerometer is mounted. A simple exemplary accelerometer, the torqued-pendulum accelerometer, is depicted in Figure 3.1. In the presence of acceleration along its sensitive axis, the pendulum tends to swing off the vertical due to a reaction torque proportional to the acceleration. A voltage proportional to the vertical angular misalignment is generated by the error-detecting coil and amplified by a high-gain amplifier. This amplified voltage is applied to the terminals of a torque-generating motor which generates a counteracting torque proportional to the applied voltage. At equilibrium, the torque generator voltage is proportional to the craft's acceleration and is the output of the accelerometer. The velocity of the craft in the direction of the sensitive axis of the accelerometer is obtained by the integration of the acceleration and the displacement of the craft, by a double integration.



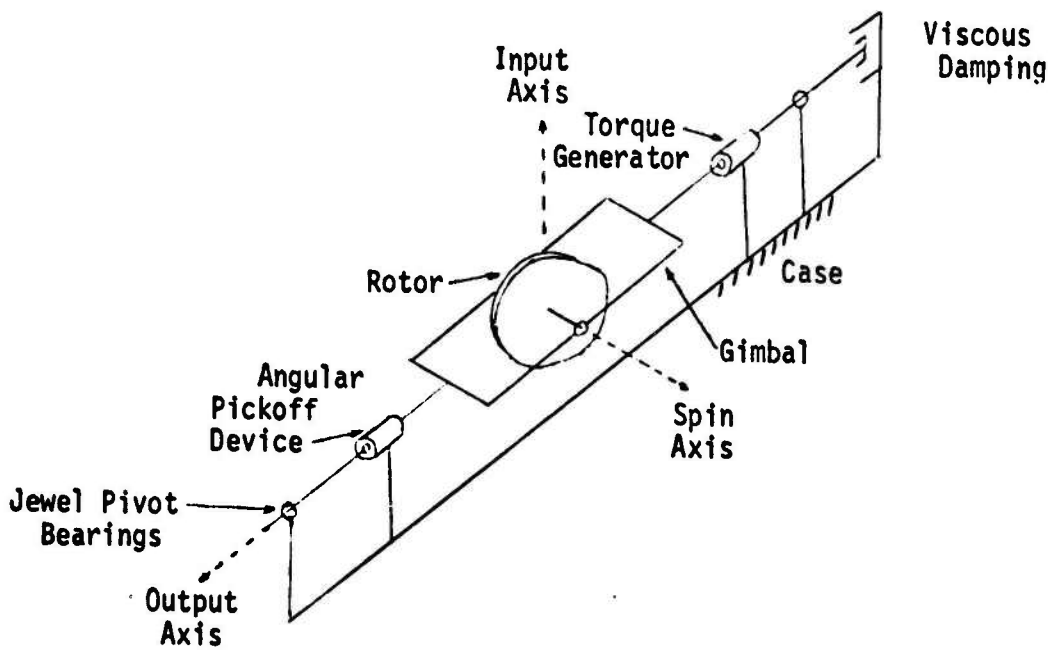
TORQUED-PENDULUM  
ACCELEROMETER

FIGURE 3.1

### Gyroscopes

The fundamental principle of all gyros lies in Newton's Second Law of motion in angular form; namely, the rate of change of angular momentum in inertial space is equal to the applied torque. A gyro is composed of a rigid body which is rotated at a high angular rate and is supported by gimbals. The angular momentum vector of the body lies in the direction of the axis about which the body spins. Angular motion which tends to change the orientation of the angular momentum vector results in the production of a torque which causes the gyro to precess (move) about an axis perpendicular to the spin axis. The precession is sensed by pickoff devices and they give an indication of the original angular motion.

In a high precision marine inertial navigation system, a particular type of gyro is employed because of its desirable characteristics. This gyro is known as a single-degree-of-freedom integrating rate gyro and is illustrated in Figure 3.2. The gyro consists of a symmetrical rotor which is rotated at a high constant rate (typically 500-1000 revolutions per second) about the spin axis. The rotor is supported by a single gimbal which is free to move about one axis, the output axis, within its case. A linear first-order viscous restraint is provided at the output axis to give the gyro its integrating rate characteristics. The gyro furnishes an output signal to rotation about only the input axis by precessing about the output axis. The precession angle (the angular movement of the spin axis about the output axis) is proportional to the angle of rotation about the input axis and is sensed by the angular pick-off device by the detection of relative angular displacements between the gyro gimbal and the supporting case. Since the precession angle is the integral of the angular rate of the case about the input axis, the gyro is



SINGLE-DEGREE-OF-FREEDOM  
INTEGRATING RATE GYRO

FIGURE 3.2

called an integrating rate gyro. This gyro also possesses the characteristic of orderly precession, that is, under the application of a torque to the output axis via the torque generator the spin axis will precess about the output axis at a rate proportional to the applied torque. In summary, a high precision integrating rate gyro can be considered as a "black box" with its input-output relationship described by Equation 3.1.

$$\omega_{OA} = A \omega_{IA} + D T_{OA} \quad (3.1)$$

where

$\omega_{OA}$  = output angular rate about the output axis,

$\omega_{IA}$  = input angular rate about the input axis,

$T_{OA}$  = control torque applied via torque generator,

A = gyro gain factor,

D = reciprocal of the viscous damping term.

#### A Damped Inertial Navigation System

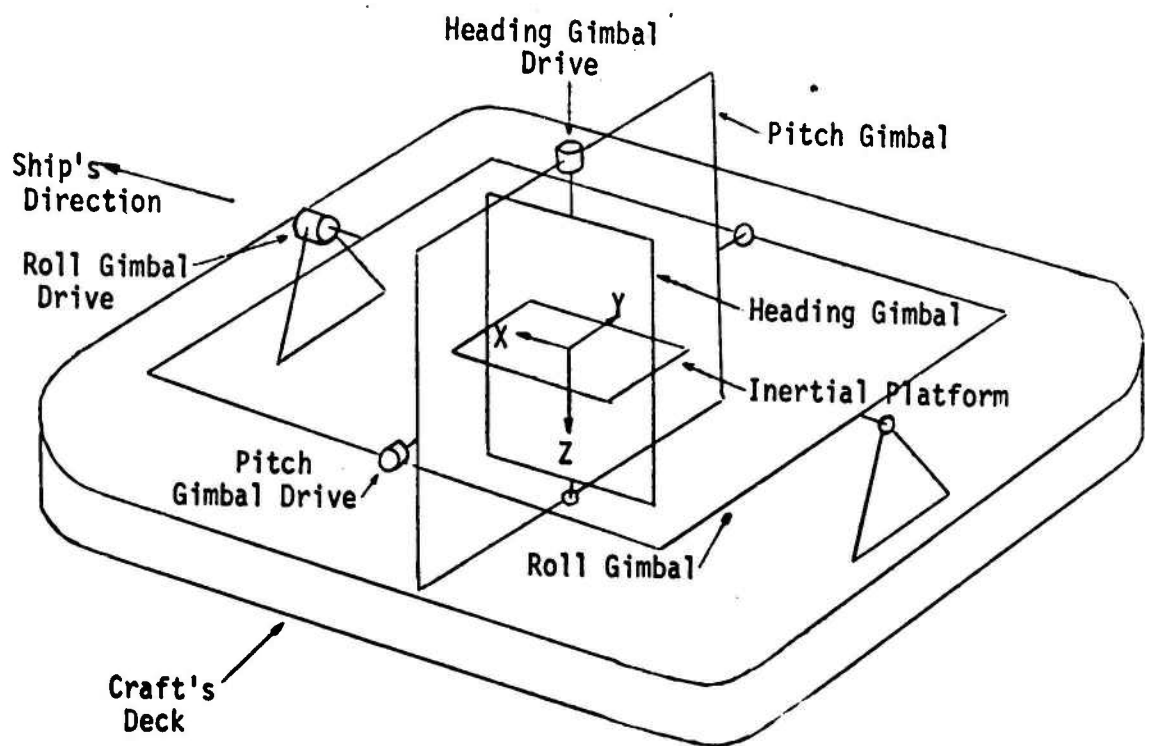
A marine inertial navigation system may have various configurations. This author has selected the one most commonly employed, namely a damped marine inertial navigation system which has a level, north-oriented platform. In this system, the platform which physically holds the inertial sensors is constantly maintained horizontal to the earth's surface with one of the accelerometer's sensitive axis directed north, the second directed east and the third directed normal to the earth's surface. The input axes of the three gyros are also aligned in this manner on the platform. The coordinate frame which the inertial sensors form is called the Geodetic Frame.

#### Platform Stabilization

To maintain this orientation of the sensors against craft's angular

motion of roll, pitch and yaw, the inertial platform is supported by three gimbals each having a servomotor drive. An illustration of the three gimbal configuration is presented in Figure 3.3. To describe the mechanism of platform stabilization against craft's angular motion, the author will consider craft's motion about the Z-axis (heading axis). The inertial platform is supported in bearings so that rotation about this axis is unconstricted. If the bearings were ideal, that is frictionless, the platform would remain unaffected by the rotational movement of the craft about the heading axis. Since this is not the case, a gyro mounted on the platform is used to sense the tendency of the platform to move about the heading axis. By employing a single-degree-of-freedom gyro with its input axis aligned along the heading axis, then any torque it receives due to the tendency of the platform to move about the heading axis will cause the gyro to precess about its output axis. To prevent platform motion, the gyro's pickoff device is used to detect the tendency of gyro-precession and to furnish a signal, properly amplified, to the heading gimbal servomotor which provides a compensation torque to the platform about the heading axis. The angle at which the heading gimbal forms with the craft's longitudinal axis yields the craft's heading angle.

In addition to platform stabilization against craft's angular motions, it is necessary for the maintenance of a level, north-oriented platform to consider craft's motion over the earth and the rotation of the earth. The angular rates associated with the craft's motion over the earth are acquired from the level accelerometers. The rates are obtained by dividing the north and east velocities by the proper radius arm and are used, after being appropriately scaled, to torque the proper gyro. The resultant gyro pickoff signal is applied to the servomotor which drives the



THREE GIMBAL  
CONFIGURATION

FIGURE 3.3

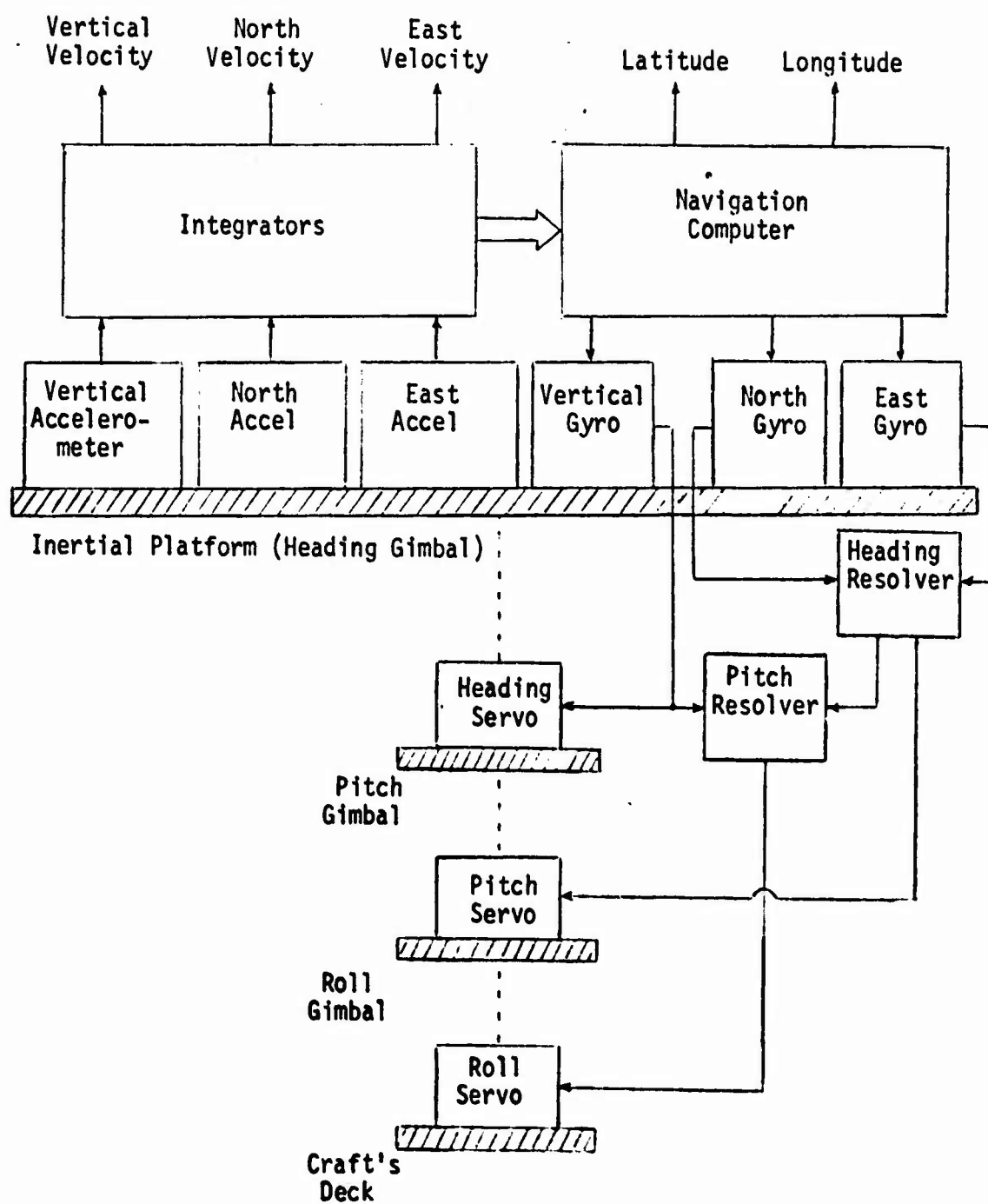
platform to maintain it horizontal. In the same manner, the navigation computer supplies the information needed to torque the gyros for the required angular rates associated with the rotation of the earth. In both cases, a high precision, linear gyro torquer is required for the proper operation of a marine inertial navigation system with a level, north-oriented platform.

#### System Function

The primary outputs of a marine inertial navigation system are craft's heading angle and craft's position given by the latitude and longitude angles. Secondary outputs are craft's north and east velocity, roll and pitch angles and vertical velocity. Figure 3.4 presents the functional diagram of a marine inertial navigation system. The heading, roll and pitch angles are obtained from the angles at which the gimbals form with the craft's deck. The function of the heading and pitch resolvers in Figure 3.4 are to calculate electronically the proportional torques required about each axis and to supply the necessary instructions to the gimbal servomotors.

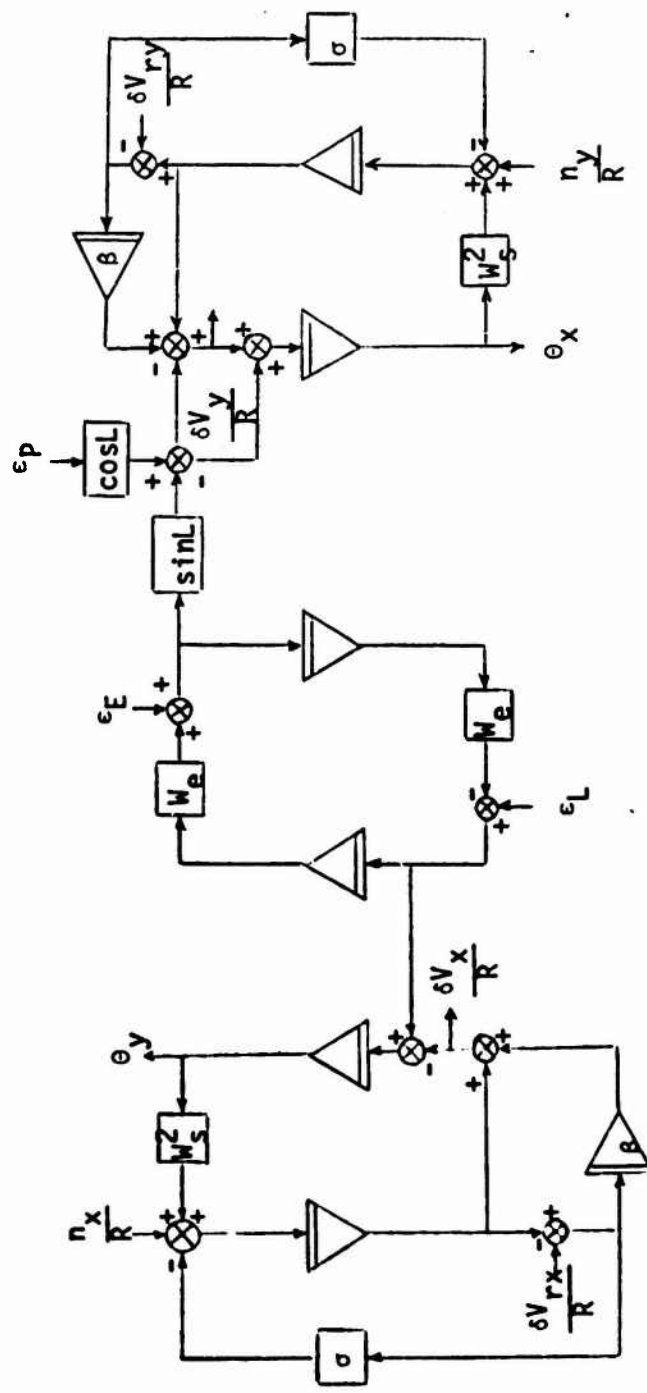
#### Error Model

In this report, a standard error model for the marine inertial navigation system was employed. Since this model can be found in much of the current literature on inertial navigation and extensive information concerning its development and its acceptability have been recorded elsewhere, References (5) and (19), this author will not expound on these topics, but will accept the model as an accurate mathematical error model of the marine inertial navigation system. The model is presented in Figure 3.5.



FUNCTION DIAGRAM OF  
MARINE INERTIAL NAVIGATION SYSTEM

FIGURE 3.4



ERROR MODEL FOR MARINE INERTIAL NAVIGATION SYSTEM

FIGURE 3.5

### System Disturbances

Disturbances to the marine inertial navigation system can be classified as:

- (1) improper initial conditions of east and north velocities, latitude, longitude and heading angles;
- (2) initial platform tilt about the north and east axes;
- (3) reference velocity errors;
- (4) accelerometer errors;
- (5) gyro drift rate errors.

All sources of error can be expressed in terms of the above disturbances. For example, the gyro drift rate error is actually composed of errors due to gyro drift bias, gyro scale factor error and gyro input axis misalignments. Gyro drift bias arises from unwanted torques from numerous sources (such as, unbalance torques, friction torques, thermal torques, etc.). Scale factor drifts are the result of any deviation in the proportionality constant relating the applied gyro torque to gyro output rate. Drifts arising from gyro input axis misalignments are due to the gyro's tendency to sense rotational rates about other axes.

### Navigation Errors

The resulting errors of interest from the above disturbances are velocity errors, tilt errors, position and heading errors. From the error model of Figure 3.5, the response or transfer functions of these output errors result in the presence of two oscillatory modes. One mode is associated with the requirement of a level platform and has a period of approximately 84.4 minutes. This period is known as the Schuler Period. The second mode results from the daily rotation of the earth and has a period of approximately 24 hours. The navigation system under study

provides damping for the first oscillatory mode. However, due to the dynamics of the navigation system, damping is not provided for the second mode. In the following chapter, the author refers to these oscillatory modes as Schuler disturbances and earth rate disturbances, respectively.

#### Need for Calibration

As mentioned in this chapter as well as Chapter I, the marine inertial navigation system is composed of six major components, namely three accelerometers and three gyros. This paper will focus on the calibration of the input axis misalignment angle in the vertical plane of a level gyro (either the X-gyro or the Y-gyro). If such a misalignment is present the level gyro will sense a portion of the rotational rates about the vertical axis. As noted earlier, in order to maintain a level, north-oriented platform, torques must be applied to the gyro to take into account the earth's rotational rate. The torque applied to the vertical gyro in this case must be such to rotate the platform about the vertical at a rate equal to  $-W_e \sin L$ . Thus the misaligned level gyro will sense an error rate equal to  $-W_e \sin \theta \sin L$  where  $\theta$  is the input axis misalignment in the vertical plane. If  $\theta$  equals 4 arc minutes and latitude equals 45 degrees, the gyro drift rate error would be 0.0124 degrees per hour. This drift rate error results in an error in latitude which oscillates indefinitely at the earth rate with an amplitude of 2.83 arc minutes (1 arc minute of latitude equals 1 nautical mile) and errors in heading and longitude which oscillate indefinitely about offsets of 4 arc minutes and 2.83 arc minutes, respectively at the earth rate with amplitudes of 4 arc minutes and 2.83 arc minutes, respectively (1 arc minute of longitude at a latitude of 45 degrees equals 0.7 nautical mile).

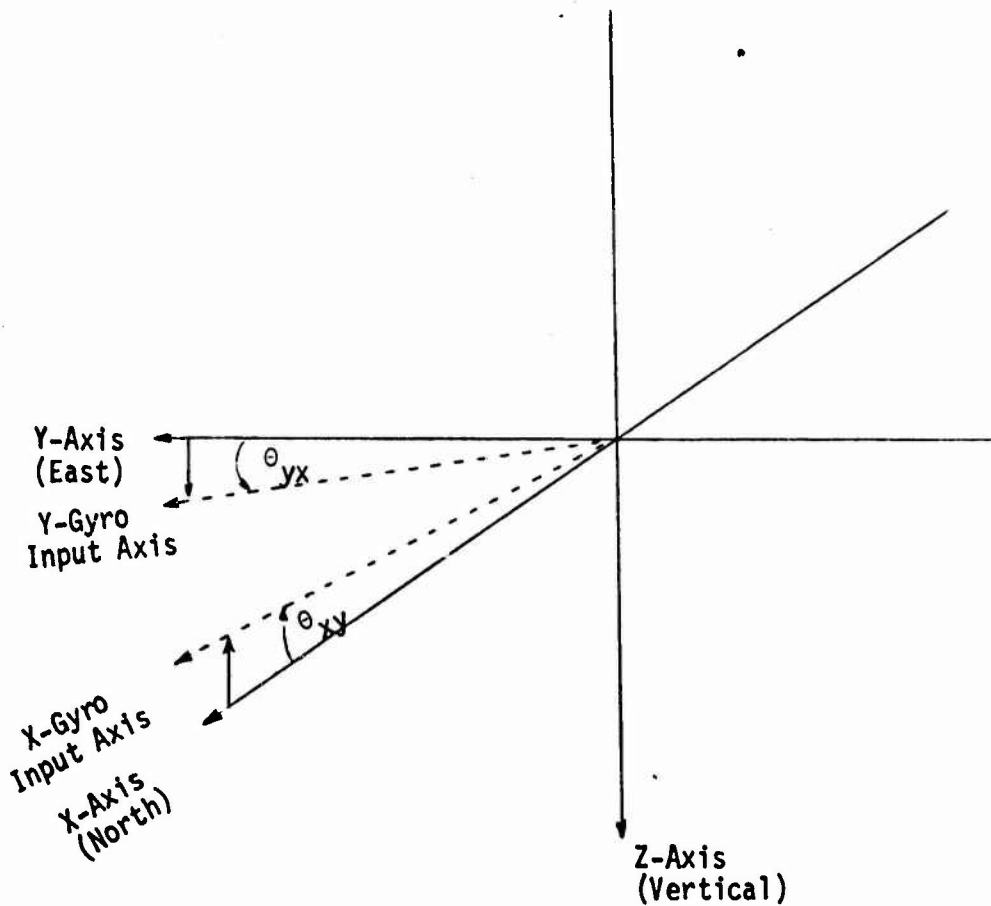
Chapter IV will present a calibration technique to determine the above gyro input axis misalignment angle. The technique requires approximately 25 minutes and can be executed while the system is performing its navigate function.

## CHAPTER IV

### CALIBRATION TECHNIQUE

In this chapter a calibration technique is presented for the east gyro (y-gyro) misalignment angle about the north-axis (in y-z plane) and for the north gyro (x-gyro) misalignment angle about the east-axis (in x-z plane) of a level, north-oriented inertial navigation platform. These misalignment angles are illustrated in Figure 4.1. The author will restrict his attention in this report to the east-gyro misalignment angle about the north-axis,  $\theta_{yx}$ . However, by symmetry the calibration procedure is equally valid for the other misalignment angle. In the ensuing discussions, the notational subscripts will be dropped and the misalignment angle will be denoted by  $\theta$ .

It has been noted in Chapter II that other calibration techniques have been developed to perform not only the calibration of these misalignment angles but also of other system parameters. The drawback of these schemes is the amount of time needed to obtain calibration results. In contrast, the calibration technique proposed in this report can be accomplished in a relatively short period of time, approximately twenty-five minutes, while the system is operating. The advantage of this report's technique becomes evident when the failure of either or both of the level gyros during mission operation is considered, namely the elimination of the downtime required by these existing schemes to calibrate the above system parameters. In addition during a long mission, calibration of these system parameters using this report's technique can be done on a periodic basis in an operate mode to insure that these parameters have not changed. This periodic procedure, however, is conditional on



GYRO INPUT AXIS  
MISALIGNMENT ANGLES

FIGURE 4.1

the need for it, namely the rate of occurrence of parameter shift.

Before proceeding to the formulation of the calibration technique, an assumption must be made that there exists a duplicate marine inertial navigation system in operation along with the system upon which calibration is being performed. The author believes that this assumption is not too prohibitive, since many missions require active redundant systems to provide uninterrupted mission operation. This is the case with regard to the marine inertial navigation system on board a United States Navy Polaris submarine. In fact, the requirement of maximum availability enforces the need for a calibration procedure in which downtime can be minimized or eliminated.

The author notes here, however, that this assumption of a redundant system may not be necessary for another calibration technique which employs the ideas presented in this report. However, further research and possible access to a marine inertial navigation system and its special operating conditions may be necessary to formulate such a calibration technique since detailed knowledge of how the input signal varies as a function of time is required.

#### Source of Perturbation

In Chapter III, it was noted that craft angular motion is sensed by the gyro and causes a tendency for the gyro to precess. This precession is detected via optical or electro-magnetic hardware and an electronic signal is generated, amplified and applied to the gimbal servo motor which prevents platform motion in inertial space. If a torque is applied to the vertical gyro, the effect is the same as if the gyro sensed craft motion about heading except that the platform does move in inertial space

about the nominal heading axis. The word "nominal" is used because if the level gyros are misaligned with respect to the horizontal plane, the horizontal stabilization mechanism of the marine inertial navigation system will keep the level gyros in whatever plane their sensitive axes form and platform rotation will be about the perpendicular axis to that plane. As the platform rotates about this non-vertical axis, the level accelerometers will begin to sense gravitational acceleration. If a constant torque is applied such that the rotational rate is  $\dot{\alpha}$  and there exists a y-gyro misalignment angle,  $\theta$ , about the x-axis, the accelerations sensed by the level accelerometers are (ignoring centrifugal effects)

$$\text{x-accelerometer: } a(t) = -g \sin(\theta) \sin \dot{\alpha}t \quad (4.1)$$

$$\text{y-accelerometer: } a(t) = g \sin(\theta) (1 - \cos \dot{\alpha}t) \quad (4.2)$$

By restricting the excursion angle,  $\dot{\alpha}t$ , to small values and for small misalignment angles we obtain

$$\text{x-accelerometer: } a(t) = -g\theta \sin \dot{\alpha}t \quad (4.3)$$

$$\text{y-accelerometer: } a(t) = 0 \quad (4.4)$$

#### Generation of Perturbation Signal

Restriction of  $\dot{\alpha}t$  to small values is accomplished by periodically applying a positive constant torque for some relatively small fixed period of time and then applying a negative constant torque for the same fixed period of time. The author has selected a torque which will provide a platform rotational rate of 120 degrees per hour. According to Reference (6), this torque is the maximum allowable torque which can be applied to the vertical gyro without incurring deteriorating effects.

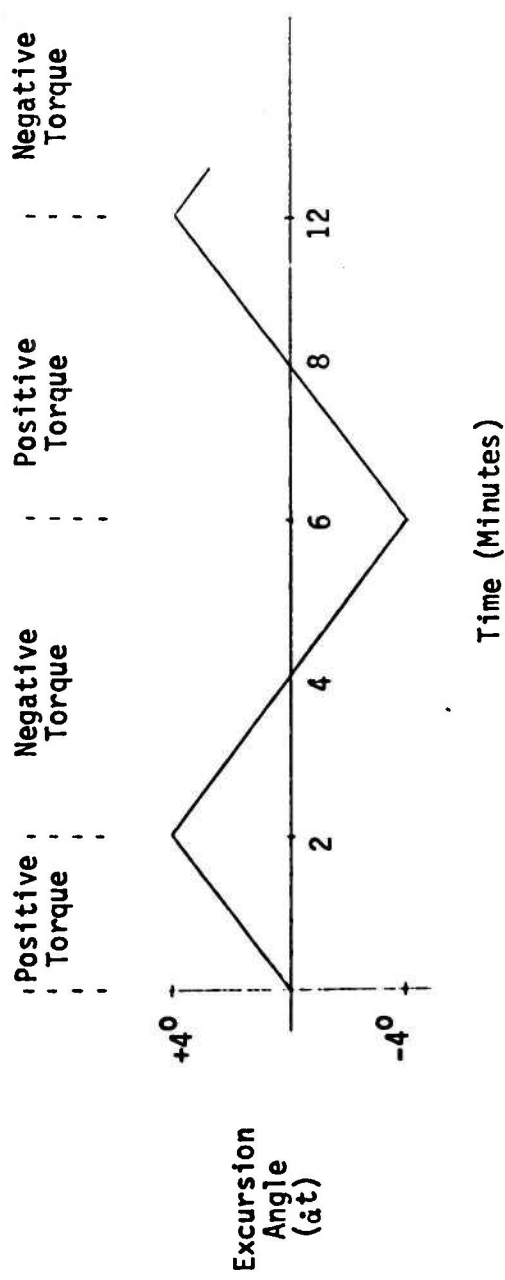
Thus initially applying this torque to the vertical gyro for two minutes

and then periodically applying negative and positive torques for four minutes results in the angle,  $\dot{\alpha}t$ , being restricted to  $\pm 4$  degrees (Figure 4.2). The periodic application of positive and negative torques is the perturbation mechanism of this report's calibration technique.

Based on Equation 4.3, this perturbation procedure gives rise to a x-axis acceleration which has a nearly triangular waveshape (Figure 4.3) and which contains the desired misalignment angle information. The system considers this acceleration as an error input, since the vehicle is not experiencing this acceleration due to actual movement. Thus, the error model presented in Chapter III can be utilized to determine the resultant velocity output. Figure 4.4 presents the portion of the error model (the x-velocity loop) now being considered. The velocity output of the model due to this "error" acceleration was determined by

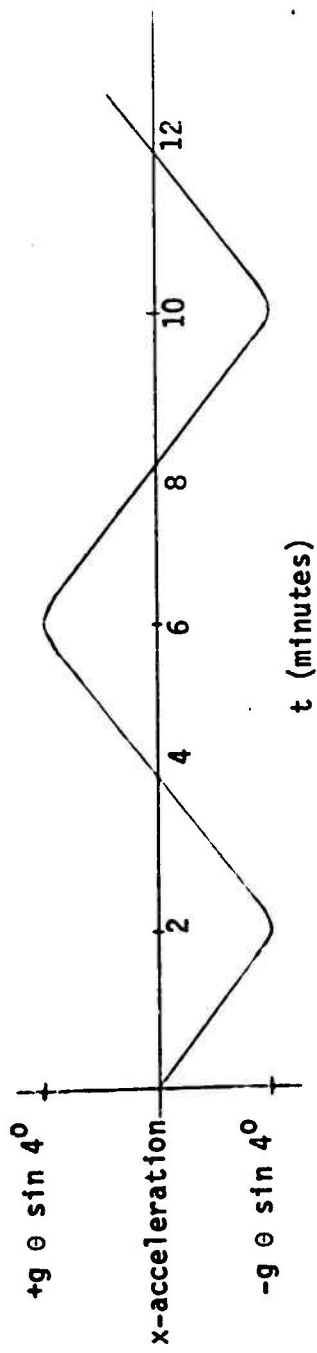
- (1) decomposing the acceleration input signal into a Fourier series,
- (2) transforming the Fourier series into Laplace transforms,
- (3) obtaining the Laplace transform of the output velocity signal by multiplying the Laplace transforms of step (2) by the Laplace transform (the transfer function) of the error model, and
- (4) finding the inverse of the Laplace transform of step (3).

In addition to the velocity output due to the "error" acceleration, there is a velocity output due to errors in the external reference velocity,  $VR$ , used to damp the system (see Figure 4.4). In the analysis, it was discovered that an undesirable input reference velocity error signal is generated by this report's perturbation procedure. However, the author found that a correction term could be calculated and added to the system's output velocity to negate the effect of this signal. The output velocity signal resulting after the application of the reference



EXCURSION ANGLE

FIGURE 4.2



THE PERTURBATION SIGNAL  
(X-AXIS ACCELERATION)

FIGURE 4.3

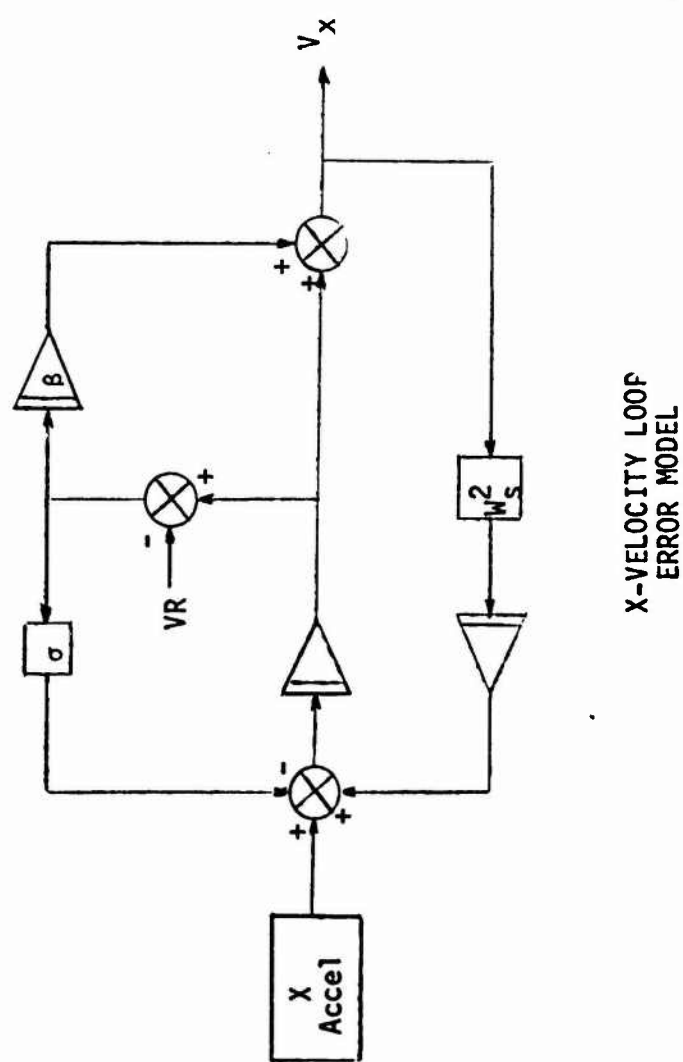


FIGURE 4.4

X-VELOCITY LOOP  
ERROR MODEL

velocity correction term is given by Equation 4.5 and illustrated in Figure 4.5. The detailed work performed by the author in arriving at Equation 4.5 is presented in Appendix A.

$$V(t) = -83.043 \theta \cos(2\pi t/T) + g(t) \quad (4.5)$$

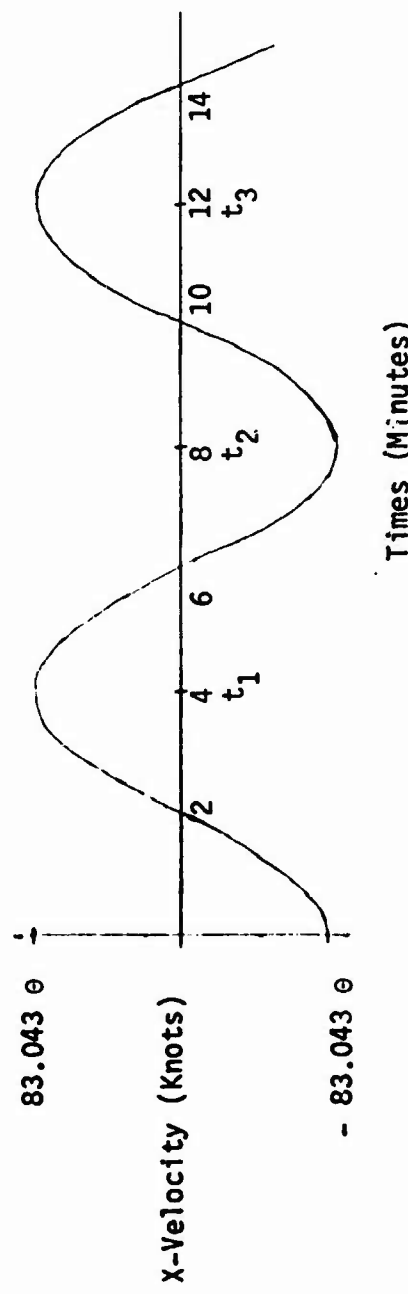
where T equals eight minutes (the perturbation period).

The second term in Equation 4.5 is composed of secondary effects which can be treated as deterministic errors in the estimation method (to be presented later in this chapter) for extracting the desired misalignment angle from the velocity data. Their resultant error contribution and the method of correction is discussed in Appendix A. For the present, the author will ignore this term and only consider the first term in Equation 4.5 in the following model development for the estimation of the misalignment angle.

#### Development of Model

##### Perturbation Effects

Velocity data is readily available from the navigation computer which records and displays the data at the end of some time interval. In this report, it is assumed that this time interval is one second. If the velocity data from the computer is sampled and stored every four minutes, a time interval equal to one-half of the perturbation period (see Figure 4.5), the velocity ideally will be equal to  $\pm 83.043 \theta$  knots. Since this observed velocity is directly proportional to the misalignment angle, it is only necessary to multiply the velocity data by a constant, K, to obtain the misalignment angle. This constant is normally referred to as a conversion factor. For example, if it is desired to obtain a value of the misalignment angle in arc minutes, we would proceed as follows:



VELOCITY OUTPUT CONTAINING  
MISALIGNMENT ANGLE INFORMATION

FIGURE 4.5

$$1 \text{ min (arc minute)} = 2.90888 \times 10^{-4} \text{ radians}$$

$$\theta \text{ min} = 83.043 \theta \text{ knots} \times K \text{ min/knot}$$

$$1/K \text{ knot/min} = 83.043 \times 2.90888 \times 10^{-4}$$

$$K \text{ min/knot} = 41.397 \text{ min/knot}$$

Thus by multiplying the observed velocity data by the above conversion factor, the result is the desired estimate in arc minutes of the misalignment angle. In the remaining discussions, the misalignment angle is considered to be in arc minutes unless otherwise stated.

#### Observation Errors

The author will now examine this estimate under practical considerations. This estimate is computed from computer samples of velocity. Let us assume that a computer velocity word contains 13 information bits as a result of resolution. Let us further assume that the most significant bit of this word is equivalent to 40 knots and therefore the least significant bit is equivalent to  $0.0097656$  knots ( $40/2^{12}$ ). Therefore the resolution that may be obtained on one estimate of the misalignment angle is 0.40 arc minutes or 24 arc seconds. Depending on the accuracy requirements of a particular system, this may be undesirable for a precision marine inertial navigation system. For example in Reference (8), typical values for the misalignment angle ranged from 9 to 12 arc seconds.

From Figure 4.5, we notice that velocity values in the vicinity of the half period velocity point are nearly constant. Thus, additional velocity data may be taken before and after this half period value and averaged to obtain a better estimate of the misalignment angle. If computer velocity data is taken over the time interval  $\pm 12$  seconds from a half period value,  $t_i$ , (see Figure 4.5) resulting in 25 velocity data

values, the average of this data would result in an estimate of 0.99555 0 which can be corrected by multiplying with a correction factor of 1.00447. This correction factor may be incorporated into the conversion factor, K, which results in a new value of 41.582.

To clarify the reasoning for the need of additional velocity data values the following example is presented. Suppose the true misalignment angle equals 3 arc minutes. This results in a velocity due to perturbation of 0.0724 knots. However, the computer velocity data word can only take on either of the following binary values:

0 000 000 000 111      corresponding to 0.068 knots

0 000 000 001 000      corresponding to 0.078 knots

These values would result in calibration errors of 10 and 14 arc seconds respectively.

Adding to this resolution problem is the inherent noise present in the accelerometer output and correspondingly in the velocity output. Averaging the velocity data reduces the effect the random noise has on the resulting calibration estimate. In addition, the author feels that the noise presence takes on a desirable characteristic. In the presence of sufficient noise randomly distributed with zero mean, the author postulates that the expected value of the computer velocity word tends to be the true velocity. In the above example if approximately 0.007 knots rms uniformly distributed noise is present, the author states that on the average 56 percent of the time the computer velocity word will be 0.068 knots and 44 percent of the time the computer word will be 0.078 knots resulting in an average of 0.0724 knots, the true velocity.

#### Outside Disturbances

Under normal operation, the vehicle containing the marine inertial

navigation system experiences accelerations in moving from one point to another. In addition, there may be schuler or earth rate disturbances in the velocity loop. To eliminate the effect of these disturbances from the velocity data, a second marine inertial navigation system is required. By subtracting the velocity of the second system from the one on which calibration is being performed, the resultant velocity is composed of the velocities due to:

- (1) the misalignment angle (Equation 4.5),
- (2) the differences in the two system's schuler and earth rate disturbances, and
- (3) the random errors present in the observed velocities.

To develop a workable model for the resultant velocity, the author states that the velocity due only to the differences in the schuler and earth rate disturbances can be approximated by a linear equation over a 20.4 minute time interval. A discussion of this approximation and its errors is deferred to Chapter V. The model for the resultant velocity is (Figure 4.6a)

$$v(t) = 83.043 \theta \cos(2\pi t/T) + a + bt + e(t) \quad (4.6)$$

where  $3.8 \leq t \leq 24.2$  minutes

Following the earlier presented procedure of observing and averaging the velocity data over the time interval  $\pm 12$  seconds from a half period value of the perturbation signal, the model can be represented in the following discrete form (Figure 4.6b)

$$v(j) = (-1)^{j+1} 81.678 \theta + A + b_j + e(j) \quad (4.7)$$

where  $j = 4, 8, 12, 16, 20, 24$  minutes

$e(j)$  = random error averaged over the time interval

$j \pm 0.2$  minutes

Figure 4.6a

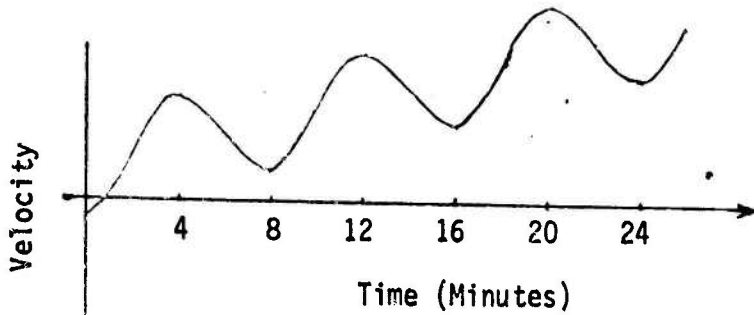
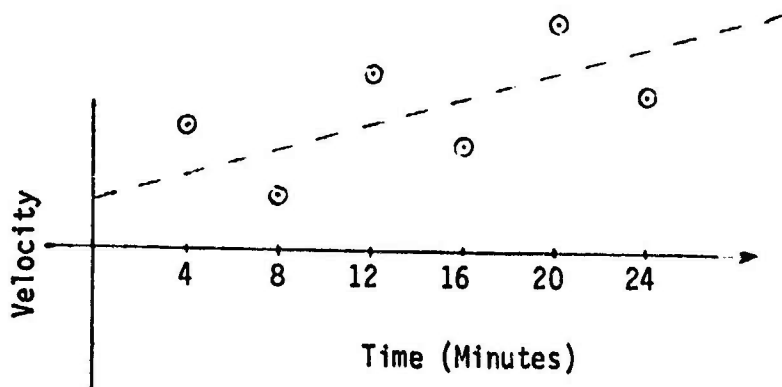


Figure 4.6b



TYPICAL VELOCITY  
OUTPUT DATA  
FOR  
ESTIMATION MODEL

FIGURE 4.6

$v(j)$  = observed velocity data averaged over the time interval,  $j \pm 0.2$  minutes

Over the proposed calibration time period of 24 minutes, six averaged velocity values are obtained. From this data, the method of least squares was used to obtain an estimate of the misalignment angle. This estimate is unbiased if the mean of the error term is constant over time (a stationary stochastic process) or if it varies linearly with time (a special non-stationary stochastic process). Further if the error term is statistically independently distributed, the estimate is a minimum variance unbiased linear estimate of the misalignment angle. The calculations involved in obtaining the estimate are presented in Appendix B. The result of these calculations for the estimate of the misalignment angle is given by Equation 4.8.

$$\hat{\theta} = K/48 (5V_1 - 11V_2 + 8V_3 - 8V_4 + 11V_5 - 5V_6) \quad (4.8)$$

where

$V_i$  = the  $i^{\text{th}}$  averaged velocity value  $i=1,2,3,4,5,6$

$K$  = conversion factor

#### Confidence Limits and Statistical Tests

To establish confidence limits for the misalignment angle and to perform statistical tests on its estimate, the author makes the assumption that the random term is an independently distributed variable. Under this assumption and by reason of the employed averaging process for the data, the author can also state that the averaged random term tends to be normally distributed due to the Central Limit Theorem of statistics (Reference 13).

If the model is correct, the  $100(1-\alpha)\%$  confidence limits for the misalignment angle are given by Equation 4.9. The detailed work in

arriving at this equation is presented in Appendix B.

$$\hat{\theta} = \hat{\theta} \pm t(3, (1-\alpha/2)) s_{\hat{\theta}} \quad (4.9)$$

where  $t(3, (1-\alpha/2))$  is the  $(1-\alpha/2)$  percentage point of the Student-t distribution with 3 degrees of freedom,

$s_{\hat{\theta}}$  is the estimated standard deviation of  $\hat{\theta}$  and can be obtained by Equation 4.10,

$$s_{\hat{\theta}}^2 = .00506K^2 \left[ \begin{array}{l} +5(v_1^2 + v_2^2 + v_5^2 + v_6^2) - 2(v_1v_5 + v_2v_6) \\ +8(v_3^2 + v_4^2 - v_1v_3 - v_2v_4 - v_3v_5 - v_4v_6) \\ -6(v_1v_2 + v_5v_6 - v_1v_6 - v_2v_5) \end{array} \right] \quad (4.10)$$

Statistical tests can also be performed on the calibration results to ascertain the statistical confidence in the calibration estimate of the misalignment angle. An example of a statistical test is now presented.

It is determined that the absolute difference between the calibration estimate and the true value of the misalignment angle should be no greater than 0.10 arc minutes with a statistical confidence of 90%. This statement is expressed in statistical terms as

$$\Pr(-.10 \leq \hat{\theta} - \theta \leq .10) \geq .90 \quad (4.11)$$

In other words, it is desired to have the probability of both events,  $(\hat{\theta} \geq \theta - .10)$  and  $(\hat{\theta} \leq \theta + .10)$ , being equal to or greater than 0.90.

$$\Pr(\theta - .10 \leq \hat{\theta} \leq \theta + .10) \geq .90 \quad (4.12)$$

Introducing the estimated standard deviation of  $\hat{\theta}$  and dividing it into the terms inside the parenthesis, we obtain:

$$\Pr(-.10/s_{\hat{\theta}} \leq (\hat{\theta} - \theta)/s_{\hat{\theta}} \leq .10/s_{\hat{\theta}}) \geq .90 \quad (4.13)$$

It has been shown in Appendix B that  $(\hat{\theta} - \theta)/s_{\hat{\theta}}$  has a student-t distribution

with 3 degrees of freedom. Therefore we have:

$$\Pr(-.10/s_\theta \leq t_3 \leq .10/s_\theta) \geq .90 \quad (4.14)$$

Noting the symmetry of the inequality (see Figure 4.7), it can be stated that for the above probability expression to be true we must have:

$$\Pr(t_3 \geq .10/s_\theta) \leq 0.05 \quad (4.15)$$

From the student-t distribution table it is observed that

$$\Pr(t_3 \geq 2.353) = 0.05 \quad (4.16)$$

Therefore

$$.10/s_\theta \geq 2.353 \quad (4.17)$$

Or

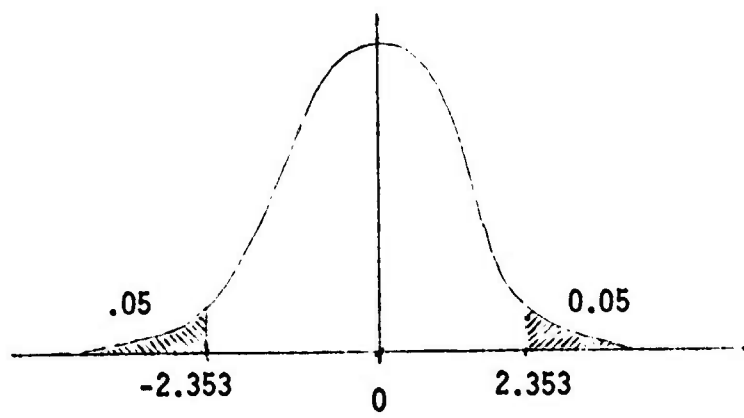
$$s_\theta \leq 0.0425 \text{ min} \quad (4.18)$$

Thus to have the stated confidence as given by Equation 4.11 in the calibration estimate, the test would require that the estimated standard deviation of the estimated misalignment angle be less than or equal to 0.0425 arc minutes.

#### Additional Estimate Efficiency

Up to this point the author has considered only one estimate of the misalignment angle. However, the calibration procedure may be continued further in time to obtain additional estimates of the system parameter. As mentioned in Chapter I, these estimates when obtained may be applied to the system to reduce the effects of large initial gyro misalignment angles. The criteria whether to apply these estimates or not can be developed from statistical tests mentioned in the preceding paragraph. These estimates may also be accumulated into a new estimate to gain better confidence in the calibration result.

For example if the calibration process were to be continued for a



STUDENT-t DISTRIBUTION  
(3 DEGREES OF FREEDOM)

FIGURE 4.7

period of time equal to  $24n$  minutes, where  $n$  is some integer, there would be available  $n$  estimates of the misalignment angle. These estimates could be combined into a new estimate as given by Equation 4.19. The new  $100(1-\alpha)\%$  confidence limits for the misalignment angle are given by Equation 4.20). The calculations for obtaining these equations are contained in Appendix B.

$$\hat{\theta} = \sum_{i=1}^n \hat{\theta}_i / n \quad (4.19)$$

$$\theta = \hat{\theta} \pm t(3n, (1-\alpha/2)) \bar{s}_{\theta} \quad (4.20)$$

where

$t(3n, (1-\alpha/2))$  is the  $(1-\alpha/2)$  percentage point of a student-t distribution with  $3n$  degrees of freedom

$$\bar{s}_{\theta} = 1/n \sqrt{\sum_{i=1}^n s_{\theta i}^2} \quad (4.21)$$

### Calibration Technique Summary

The report's calibration technique for a marine inertial navigation system is presented below in a step-by-step format:

- (1) Commencement. Initiate the calibration procedure at some time,  $T$ , while the system is operating.
- (2) Inducement of a Perturbation Signal. Initially apply a positive torque (causing the inertial platform to rotate at a rate of 120 degrees per hour) to the vertical gyro for a period of two minutes and then periodically apply negative and positive torques

to the vertical gyro for a time interval of four minutes each.

- (3) Observation of Perturbation Signal Effect. At times equal to  $T + (3.8+t)$  minutes, where  $t = 0, 4, 8, 12, \dots$  observe the output of the north/east velocity of both navigation systems at one second intervals for a period of 24 seconds. The misalignment angle is contained in the north velocity if the east gyro is misaligned and in the east velocity if the north gyro is misaligned.
- (4) Removal of Reference Velocity Effect. For each velocity data value from the system which is being calibrated, compute the reference velocity correction term and add this term to the velocity data value of that system.
- (5) Isolation of Perturbation Signal Effect. Compute the difference between the two systems' velocity data values and average them over the 24 second time interval.
- (6) Estimation of Misalignment Angle. After six averaged difference velocity terms have been collected, compute the estimate for the misalignment angle by Equation 4.8.
- (7) (Optional) Enhancement of Estimate. If increased efficiency is desired, obtain additional estimates via steps 3, 4, 5 and 6. Compute the more efficient estimator by Equation 4.19.
- (8) Termination. After the desired final velocity data value has been observed, apply a torque to the vertical gyro to bring the system back to normal operation and insert the calibrated system parameter into its proper location in the navigation computer.

### Discussion of Calibration Technique

The author now directs his attention to some of the general problematic areas presented in Chapter I.

First, is any additional hardware needed to accomplish the calibration procedure? As observed from the preceding summary section, the procedural steps require data observation, data computation, timing control and the capability of applying torques to the vertical gyro. All of these operations are already performed and/or directed by the on-board navigational computer. However, a computer program is required to direct the navigational computer to complete these specific tasks.

Second, is the model for the observed velocity data correct? The author believes that the model presented in this report will accurately represent the observed data and will lead to the proper estimation of the misalignment angle. However, to confirm the validity of the model, actual velocity data is required. This data need not be obtained during the actual application of the calibration technique but can be acquired under normal operating conditions. Statistical tests to confirm the validity of the model are presented in References (3) and (9). Once the validity of the model is confirmed, the "goodness" of the estimate may be ascertained by analyzing the random error term to determine its distribution and possible correlation function. References (14) and (16) may be employed to assist the analyst in this task.

Third, how often does the system parameter which is being calibrated change? This report's calibration technique obtains an estimate of the misalignment angle in approximately 25 minutes. However, continuation of the procedure for a period of from one to two hours may be necessary to obtain a better estimate. In any event although the rate of occurrence

of parameter shift is unknown to the author, it is evident that this report's calibration technique is superior with regard to possible parameter shift to the calibration procedures presented in Chapter II, in that the time for parameter calibration is significantly reduced.

Fourth, is it physically possible to observe the output signal at the times required by the calibration technique? As noted earlier in this chapter, one of the functions of the navigational computer is to periodically observe and display the velocity data which, for this report's technique, contains the misalignment angle information. The frequency of observation is dependent upon the equipment capabilities and the actual needs of a particular navigation system. The author has assumed that the navigational computer possesses the capability of observing velocity data every second. This he believes is a reasonable assumption, but if for a particular system it proves false, reduction in the number of velocity data values used in the averaging process may be required.

Fifth, will the dynamics of the system prevent the insertion of the perturbation signal? At what magnitude of the perturbation signal will system operation degenerate? The application of torques to the vertical gyro is the perturbation mechanism of this report's calibration technique. The author selected a torque which provided for minimum calibration time while maintaining the gyro torquer in its linear range of operation. This selection was based on gyro torquer evaluation studies performed in Reference (6). According to their studies "no gyro torquer has been more non-linear than 0.06% RMS, with many torquers exhibiting non-linearities of less than 0.01%" over a range of platform rotation rates,  $\pm 120$  degrees per hour.

The author also performed investigations into the centripetal and

tangential accelerations resulting from the induced angular velocity and angular acceleration, respectively, of the rotating inertial platform. The velocity signals generated by these accelerations in addition to being small were mitigated by the estimation process by reason of their 90 degree phase relationship with the velocity signal containing the misalignment angle information. Their resultant error contribution to the estimation of the misalignment angle was negligible.

The period and amplitude of the perturbation signal (Figure 4.3) for his report's calibration technique was selected after proper consideration was given to the time of calibration, the perturbation resultant velocity, the error produced by the perturbation signal and to the capability of ideally detecting a one second misalignment angle. The acceptability of this selection is addressed in the following chapter where an error analysis of the calibration technique is formulated.

## CHAPTER V

### ERROR ANALYSIS

The chapter presents the errors developed in the primary marine inertial navigation system outputs when this report's calibration procedure is employed. The errors are divided into two categories, namely the errors caused by an uncalibrated gyro input axis misalignment parameter and the errors induced into the system by the calibration technique. An investigation into possible sources of error in the calibration results is also presented. The feasibility of the proposed calibration technique is primarily dependent on the results of this error analysis.

#### Uncalibrated Parameter Error

As noted in Chapter III, the error due to an uncalibrated level gyro input axis misalignment in the vertical plane is equivalent to a level gyro drift rate error of  $(15 \theta \sin L)$  degrees per hour, where  $\theta$  is the misalignment angle and  $L$  is the latitude position of the vehicle. For example, if  $\theta$  equals 1 arc minute and latitude equals 45 degrees, then the level gyro drift rate error is 0.0031 degrees per hour. Employing the error model presented in Chapter III, the author calculated the primary output errors resulting from this system disturbance using Laplace Transforms. The errors (as a function of latitude and the uncalibrated parameter) developed in the primary marine inertial navigation system outputs 25 minutes after the system has been placed into an operate mode are presented in Table 5.1. The table is divided into two sections since the system errors developed are functions of the particular gyro (east or north) being calibrated. Table 5.2 presents the system errors for a gyro

TABLE 5.1

NAVIGATION ERRORS -  
UNCALIBRATED PARAMETER

	East Gyro Calibration	North Gyro Calibration
$\delta L$	$0.0431 \theta \sin L$	$0.0013 \theta \sin^2 L$
$\delta \lambda$	$0.0013 \theta \sin L \tan L$	$-0.0431 \theta \tan L$
$\delta H$	$0.0011 \theta \sin 2L$ $+0.0038 \theta \tan L$	$-0.0431 \theta \sin L \tan L$

TABLE 5.2

NAVIGATION ERRORS -  
UNCALIBRATED PARAMETER  
OF ONE ARC MINUTE  
AT A LATITUDE OF 45 DEGREES

	East Gyro Calibration	North Gyro Calibration
$\delta L$	0.030 min	0.001 min
$\delta \lambda$	0.001 min	-0.043 min
$\delta H$	0.005 min	-0.030 min

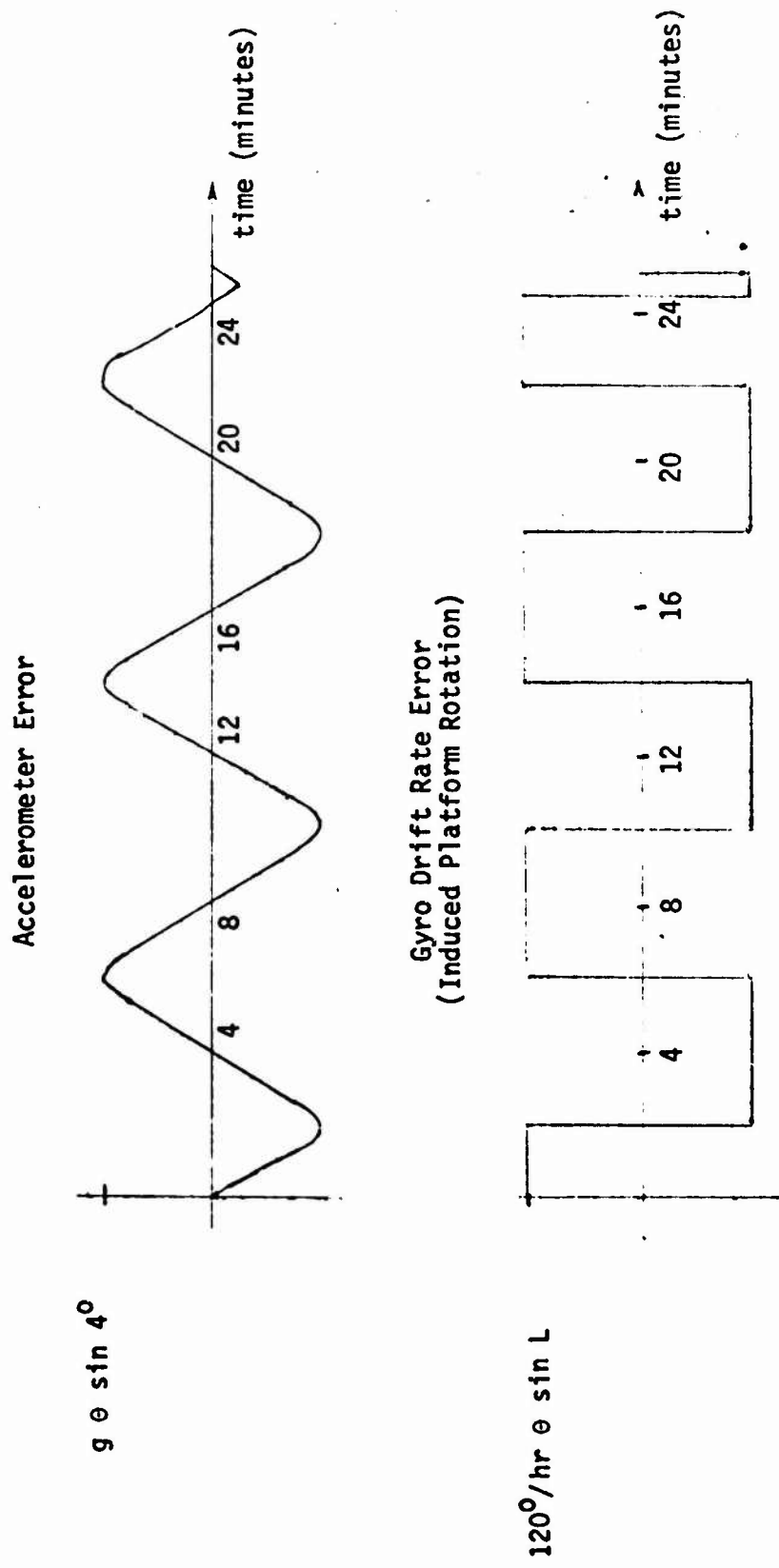
misalignment angle of one arc minute and a latitude of 45 degrees. After conversion, the maximum developed error for the above case results in a positional error of 183 feet. The author believes this error is tolerable for a precision marine inertial navigation system for two reasons. First, the developed error besides being small is present for a relatively short period of time, 25 minutes. Second, since the error is deterministic upon knowledge of the gyro parameter, the developed error may be removed upon completion of the calibration procedure.

#### Calibration Induced Error

The system error disturbances resulting from the calibration technique fall into three categories:

- (1) accelerometer disturbance,
- (2) gyro drift rate disturbance, and
- (3) cross-axis gyro drift rate disturbances.

The accelerometer disturbance is the induced perturbation signal used by the calibration technique to calibrate the desired gyro parameter. The gyro drift rate disturbance is similar to the drift rate error caused by the uncalibrated parameter. It originates from the periodic application of positive and negative torques to the vertical gyro causing the platform to rotate at the rates of  $\pm 120$  degrees per hour. These two system error disturbances are illustrated in Figure 5.1. The cross-axis gyro drift rate disturbances result from the other gyro which is not being calibrated being driven out of the horizontal plane by the calibration technique in the same manner as its corresponding accelerometer which produces the perturbation signal. This causes the gyro to sense a portion of the platform rotational rates, namely the earth rate and the



ACCELEROMETER AND GYRO  
DRIFT RATE ERRORS

FIGURE 5.1

calibration induced rate of  $\pm 120$  degrees per hour. These cross-axis system error disturbances are illustrated in Figure 5.2.

The calibration procedure induced errors developed in the primary system outputs after 25 minutes are presented in Tables 5.3, 5.4, 5.5 and 5.6. Table 5.7 presents the total navigational errors resulting from the calibration technique. Table 5.8 presents the navigational errors for a gyro misalignment angle of one arc minute at a latitude of 45 degrees. These errors are of the same magnitude as those caused by the uncalibrated parameter and for the same reasons are believed to be tolerable.

#### Error in Calibration Results

When the author in Chapter IV developed the velocity model for obtaining an estimate of the calibration parameter, he assumed that the differences in the schuler and earth rate disturbances could be approximated by a linear equation over a 20.4 minute time interval. Considering the earth rate disturbance, this approximation is extremely good since earth rate disturbances, as noted in Chapter III, oscillate with a period of 24 hours. The maximum error which a one knot uncommon earth rate disturbance could contribute to the calibration result based on this report's model is 0.004 arc seconds. However, this is not the case with the schuler disturbances which for our system have a damped oscillation with a period of approximately 90 minutes. Depending on the time of origination, a one knot uncommon schuler disturbance could contribute as much as an 8 arc second error in this report's calibration result. Two courses of action are open if a large uncommon schuler disturbance is present in the systems and if a change in the calibration technique is

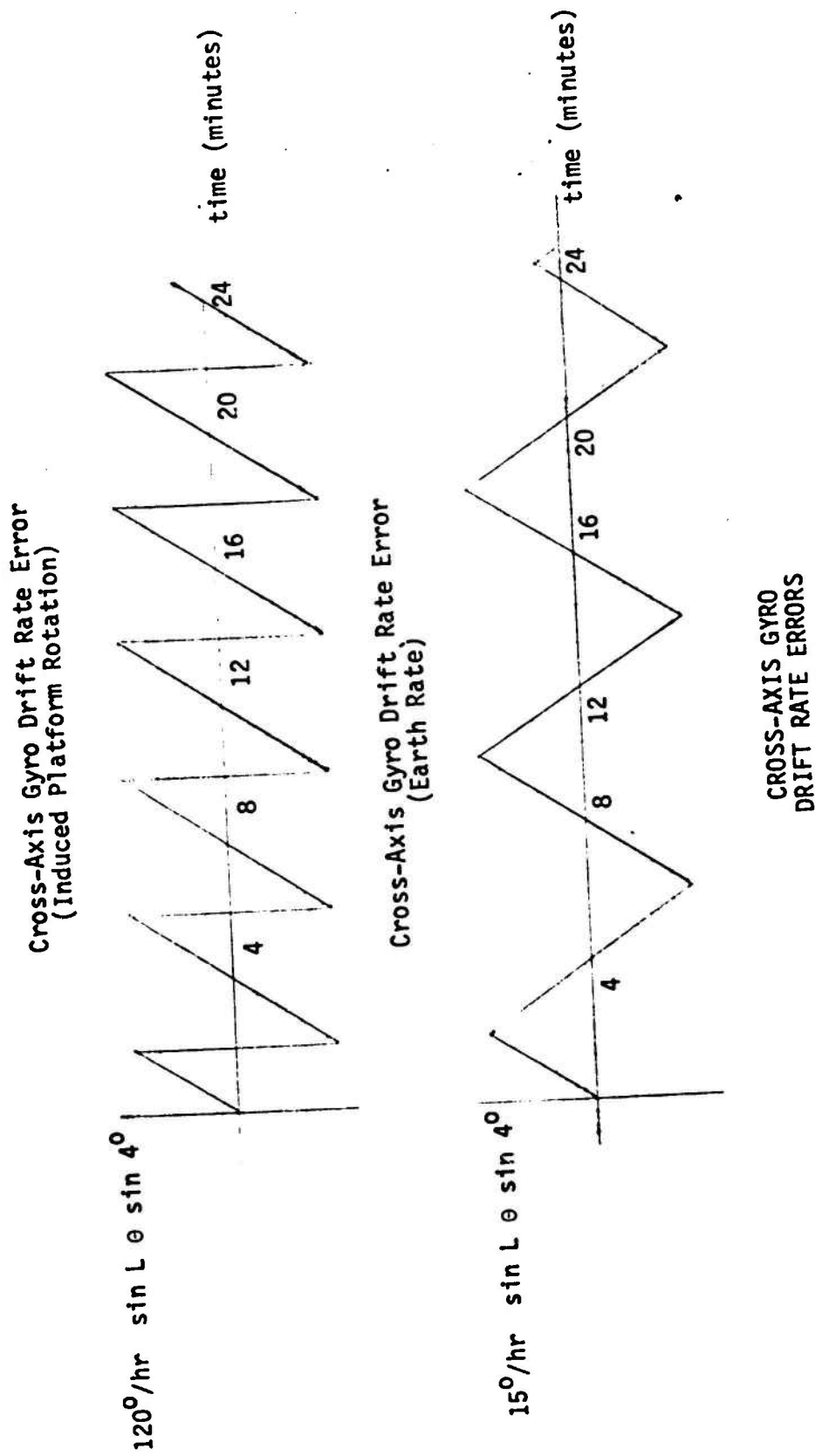


FIGURE 5.2

TABLE 5.3

NAVIGATION ERRORS -  
INDUCED ACCELERATION DISTURBANCE

	East Gyro Calibration	North Gyro Calibration
$\delta L$	0.0062 $\theta$	0.0
$\delta \lambda$	0.0	-0.0062 $\theta \tan L$
$\delta H$	0.0	-0.0062 $\theta \sec L$

TABLE 5.4

NAVIGATION ERRORS -  
GYRO DRIFT RATE DISTURBANCE

	East Gyro Calibration	North Gyro Calibration
$\delta L$	0.0052 $\theta \sin L$	0.0003 $\theta \sin^2 L$
$\delta \lambda$	0.0003 $\theta \sin L \tan L$	-0.0052 $\theta \tan L$ -0.0006 $\theta \sin 2L$
$\delta H$	0.0001 $\theta \sin 2L$ +0.0003 $\theta \tan L$	-0.0045 $\theta \sin L \tan L$

TABLE 5.5

NAVIGATION ERRORS -  
 CROSS-AXIS GYRO DRIFT RATE  
 (INDUCED PLATFORM ROTATION)

	East Gyro Calibration	North Gyro Calibration
$\delta L$	$0.0299 \theta \sin L$	$0.0015 \theta \sin^2 L$
$\delta \lambda$	$0.0015 \theta \sin L \tan L$	$-0.0074 \theta \sin 2L$ $-0.0150 \theta \tan L$
$\delta H$	$0.0008 \theta \sin 2L$ $+0.0015 \theta \tan L$	$-0.0299 \theta \sin L \tan L$

TABLE 5.6

NAVIGATION ERRORS -  
 CROSS-AXIS GYRO DRIFT RATE  
 (EARTH ROTATIONAL RATE)

	East Gyro Calibration	North Gyro Calibration
$\delta L$	$0.0004 \theta \sin L$	$0.00002 \theta \sin^2 L$
$\delta \lambda$	$0.00002 \theta \sin L \tan L$	$-0.0004 \theta \tan L$
$\delta H$	$0.00002 \theta \tan L$ $+0.00001 \theta \sin 2L$	$-0.0004 \theta \sin L \tan L$

TABLE 5.7  
TOTAL NAVIGATION ERRORS -  
CALIBRATION TECHNIQUE

	East Gyro Calibration	North Gyro Calibration
$\delta L$	$0.0062 \theta$ $+0.0355 \theta \sin L$	$0.0020 \theta \sin^2 L$
$\delta \lambda$	$0.0018 \theta \sin L \tan L$	$-0.0268 \theta \tan L$ $-0.0080 \theta \sin 2L$
$\delta H$	$0.0018 \theta \tan L$ $+0.0009 \theta \sin 2L$	$-0.0062 \theta \sec L$ $-0.0348 \theta \sin L \tan L$

TABLE 5.8  
TOTAL NAVIGATION ERRORS -  
CALIBRATION TECHNIQUE  
 $\theta = 1$  arc minute  
 $L = 45$  degrees

	East Gyro Calibration	North Gyro Calibration
$\delta L$	0.031 min	0.001 min
$\delta \lambda$	0.001 min	-0.035 min
$\delta H$	0.003 min	-0.033 min

not desired. First, the initiation of the calibration technique could be delayed until the magnitude of the uncommon schuler disturbance is mitigated by the system damping. Second, the calibration procedure could be continued until four estimates of the system parameter have been obtained. This latter course of action will insure that the error caused by an uncommon schuler disturbance as large as one knot will be less than one arc second.

## CHAPTER VI

### CONCLUSIONS

In the preceding chapters, the author has formulated and investigated a calibration technique which is performed in an operate mode for a particular system. The author believes that this study indicates the feasibility of such a calibration technique. In particular, the system errors caused by operation with an uncalibrated system parameter and by the disturbing effects of the calibration technique were shown in the author's view to be tolerable. However, although the author has attempted to mitigate the effect of system noise on the calibration results, additional information concerning the quantity and quality of noise present in the system outputs is needed for complete confirmation of the report's particular calibration technique.

Although this report presented a calibration technique for a specific system, a similar technique employing the ideas and concepts presented in this report may be developed for other systems to reduce or eliminate their calibration downtime. The formulation of such a technique is especially desirable for systems whose unavailability at a time of critical need could result in a catastrophic loss of men, material and tactical advantage.

Besides the obvious feature of the reduction of total system downtime, the calibration technique displays the feature of automatic calibration wherein data for calibration results are obtained from actual system outputs via the controlling computer, thus alleviating the need for external measuring instruments such as meters, collimators, theodolites, etc. Repeated measurements may easily be taken and statistical tests employed

to determine the "goodness" of the results.

In addition, there is a secondary effect of this type of calibration, namely an insight into system performance. By the very nature of the calibration's procedure of perturbation, the dynamic performances of the system components are exercised with predictable consequences. Thus, marginal components which might otherwise go undetected may be discovered by monitoring their outputs for unusual behavior during the calibration procedure. This secondary effect has a greater bearing on maintainability than one would assume at first. First, this advanced knowledge of possible system failure will prepare the operator for possible replacement of the marginal component when the system is not required for mission operation, thus preventing a possible failure during a future mission. Second, in the event of a system failure, this advanced knowledge may lead to a reduction of active repair time needed for trouble shooting procedures. Third, if immediate replacement of the marginal component is unnecessary, a replacement for this component may be ordered in advance, thus reducing logistic downtime. These additional benefits derived from the employment of a calibration technique performed in an operate mode should be investigated by the responsible engineer when this type of calibration is selected for a particular system.

## REFERENCES

1. Arnold, Ronald N. and Leonard Maunder. Gyrodynamics and Its Engineering Applications. Academic Press, New York and London, 1961.
2. Blanchard, Benjamin S. and E. Edward Lowery. Maintainability. McGraw-Hill Book Co., New York, 1969.
3. Bowker, Albert H. and Gerald J. Lieberman. Engineering Statistics. Prentice-Hall, Inc., Englewood Cliffs, New Jersey, 1972.
4. Britting, Kenneth P. Inertial Navigation System Analysis. John Wiley and Sons, Inc., New York, 1971.
5. Caligiuri, J.F. "Analysis of Pure and Augmented Inertial Navigation Systems," Collected notes from Space course at Sperry Systems Management, Great Neck, New York.
6. Cilo, Mark P. and Ronald S. Vaughn. "A New Technique for Simultaneous East Angular Sensor Calibration and Navigation of Inertial Systems," Dept. of the Navy, Naval Air Development Center, Johnsville, Pa., Report No. NADC-AM-6722, 13 December 1967.
7. Del Toro, Vincent and Sydney P. Parker. Principles of Control Systems Engineering. McGraw-Hill Book Co., Inc., New York, 1960.
8. Diamond, Warren and Herbert Seligman. "MK 3 MOD 4 SINS/Investigation of the Navigate Theta D. Gyro Calibration Technique (U)," U.S. Naval Applied Science Laboratory, Brooklyn, New York, Lab. Project 950-21, Progress Report 3, 7 March 1968.
9. Draper, N.R. and H. Smith. Applied Regression Analysis. John Wiley and Sons, Inc., New York, 1966.
10. Geller, E.S. "Inertial System Platform Rotation," IEEE - Transaction on Aerospace and Electronic Systems, Vol. AES-4, No. 4, July 1968.
11. General Precision, Inc. "Calibration of Gyros at Sea (U)," Contract No. AF04(694)119, Little Falls, New Jersey, 19 April 1963.
12. General Precision, Inc. "Fourth Gyro Investigation (II)," Contract No. AF04(694)119, Little Falls, New Jersey, 15 November 1962.
13. Hald, A. Statistical Theory with Engineering Applications. John Wiley and Sons, Inc., New York, 1965.
14. Hicks, Charles R. Fundamental Concepts in the Design of Experiments. Holt, Rinehart and Winston, New York, 1973.
15. Javid, Mansour and Egon Brenner. Analysis, Transmission and Filtering of Signals. McGraw-Hill Book Co., New York, 1963.

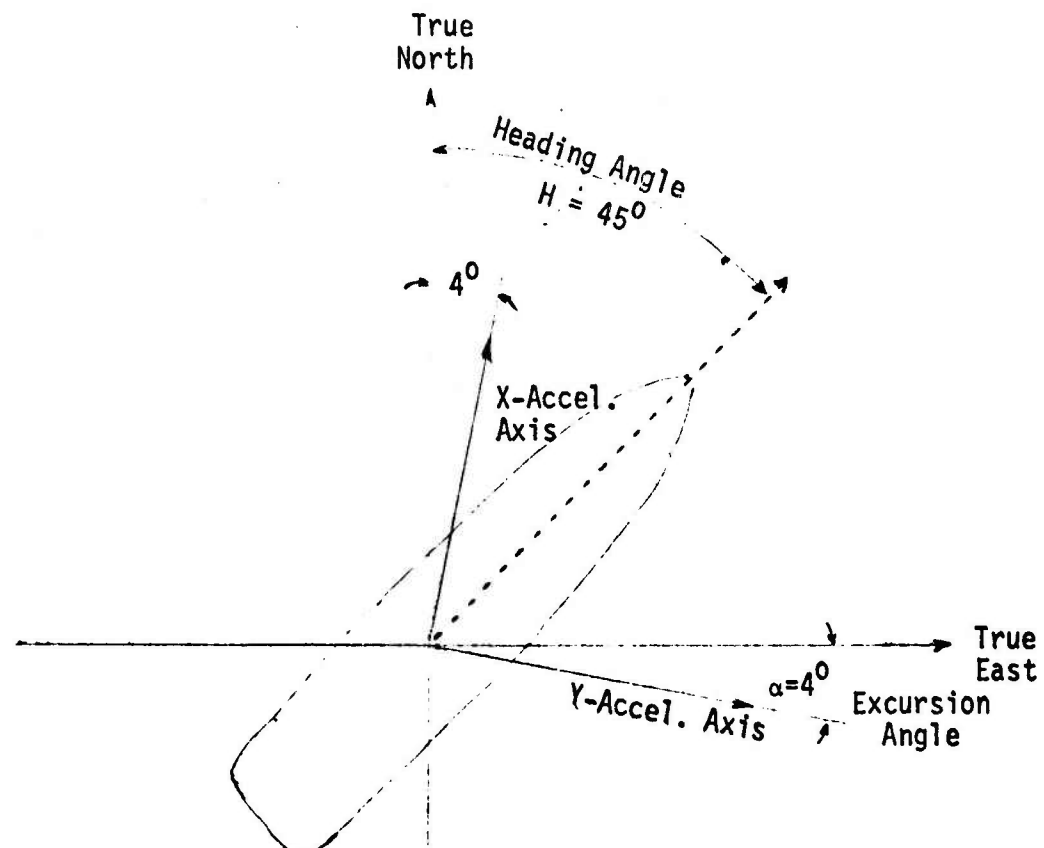
16. Jenkins, Givilyn M. and Donald G. Watts. Spectral Analysis and Its Applications. Holden-Day, Inc., San Francisco, 1968.
17. Leff, Edward. "Procedure - Automatic Calibration for Gyros and Vibrating String Accelerometers at Sea (U)," Contract No. AF04 (694)119, General Precision, Inc., Little Falls, New Jersey, 28 June 1963.
18. Murray, A.R.M. "Inertial Navigation." Industrial Electronics, Vol. 2, No. 7, July 1964.
19. O'Donnell, C.P. Inertial Navigation Analysis and Design. McGraw-Hill Book Co., New York, 1964.
20. Savet, Paul H. Gyroscopes: Theory and Design. McGraw-Hill, New York, 1961.

## APPENDIX A

This appendix investigates the effect that a reference velocity error has on the estimation of the misalignment angle and shows that this effect can be negated by the addition of a correction term to the observed velocity. The resulting corrected velocity containing the misalignment angle information is analytically determined using the Fourier Series Theorem and Laplace Transforms. The resulting analytic expression for this velocity is divided into a pure perturbation signal term and into secondary effects. Chapter IV uses the pure perturbation signal term in the development of an estimation method for the misalignment angle. The secondary effects are treated in this appendix with respect to their error contribution to the estimation of the misalignment angle. Compensation for their effect is also discussed.

The marine inertial navigation system obtains the reference velocity for damping purposes by the employment of an electro-magnetic log (EM LOG) which measures the speed of the vehicle through the water. This velocity is resolved through the heading and excursion angle (Equation A.1) before being applied to the system. For example if at some time the heading angle (the angular position of the vehicle relative to the direction of north) is 45 degrees, the excursion angle is 4 degrees and the EM LOG has a reading of 10 knots, the reference velocity applied to the Y-velocity loop would be 6.56 knots ( $10 \sin(45-4^\circ)$ ) and that applied to the X-velocity loop would be 7.55 knots ( $10 \cos(45-4^\circ)$ ). An illustration of this example is presented in Figure A.1.

$$\begin{aligned} VR_x &= VR \cos(H-\alpha) \\ VR_y &= VR \sin(H-\alpha) \end{aligned} \tag{A.1}$$



## REFERENCE VELOCITY RESOLUTION

FIGURE A.1

where  $H$  = heading angle

$\alpha$  = excursion angle

If the reference velocity is in error by  $dVR$  while the platform is rotated at a rate of  $\dot{\alpha}$ , 120 degrees per hour, and if a heading error  $dH$  is present the resulting reference velocity error applied to the X-velocity loop is

$$dVR_x = \begin{bmatrix} (VR+dVR) dH \cos H \sin \dot{\alpha} t + dVR \sin H \sin \dot{\alpha} t \\ -(VR+dVR) dH \sin H \cos \dot{\alpha} t + dVR \cos H \cos \dot{\alpha} t \end{bmatrix} \quad (A.2)$$

It is noted that the first and second terms of Equation A.2 are of the same form as the perturbation signal of this report's calibration technique repeated in Equation A.3 and thus are indistinguishable from the perturbation signal containing the misalignment angle information.

$$a_x = -g \theta \sin \dot{\alpha} t \quad (A.3)$$

To negate the effect of this undesirable reference velocity error signal, the author has determined by an investigation of the error model that the addition of the output, denoted by  $V_3$  in Figure A.2, of the third order integrator multiplied by the constant  $(\alpha/\beta - 1)$  to the system velocity output produces the desired results. Working in Laplace Transforms, we have for the uncorrected velocity output

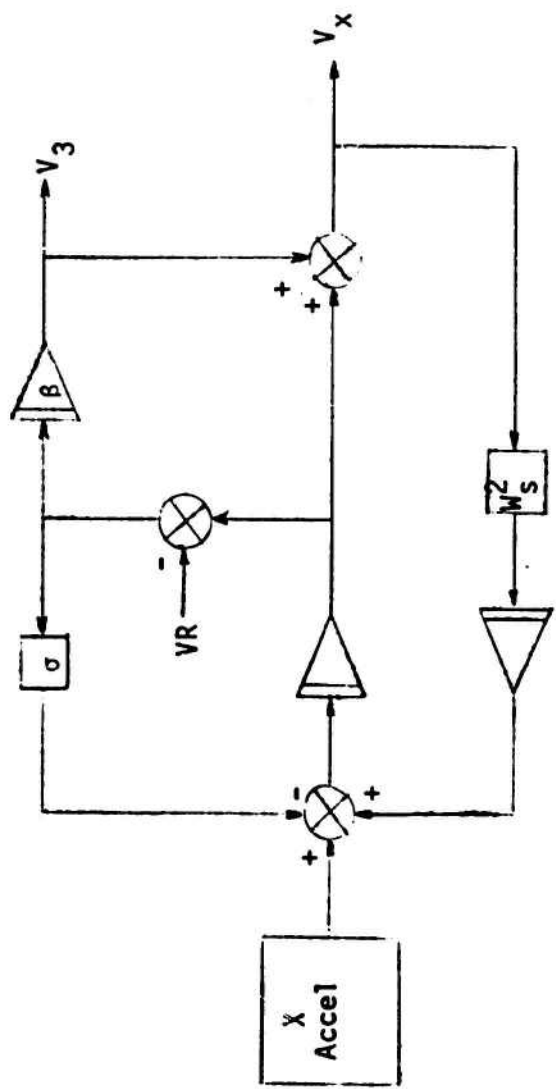
$$V_x = \frac{s^2 + \beta s}{D(s)} A_x + \frac{(\alpha - \beta) s^2}{D(s)} VR_x \quad (A.4)$$

$$\text{where } D(s) = s^3 + \alpha s^2 + W_s^2 s + \beta W_s^2$$

and for the output of the third order integrator

$$V_3 = \frac{\beta s}{D(s)} A_x - \frac{\beta s^2 + \beta W_s^2}{D(s)} VR_x \quad (A.5)$$

Multiplying the output of the third order integrator by  $(\alpha/\beta - 1)$ , we



VELOCITY ERROR MODEL

FIGURE A.2

obtain the correction term

$$(\sigma/\beta - 1)V_3 = \frac{(\sigma-\beta)}{D(s)} s A_x - \frac{(\sigma-\beta) s^2 + (\sigma-\beta) W_s^2}{D(s)} V_{R_x} \quad (A.6)$$

and adding this correction term to the velocity output

$$V_x \text{ (corrected)} = \frac{s^2 + \sigma s}{D(s)} A_x - \frac{(\sigma-\beta) W_s^2}{D(s)} V_{R_x} \quad (A.7)$$

In effect by use of this correction factor, the author has reduced the resultant error of the reference velocity by the factor  $W_s^2/s^2$  where  $s$  equals the frequency of the perturbation signal (47.12 radians/hour) and  $W_s$  equals the Schuler Frequency (4.4667 radians/hour).

Analysis of the effect of heading and reference velocity errors after the correction term has been applied has shown that the error introduced into the estimation of the misalignment angle can be expressed as

$$\theta \text{ (error in sec)} = 1.18 \left[ (V_{R_x} + dV_{R_x}) dH \cos H + dV_{R_x} \sin H \right] \quad (A.8)$$

For example, traveling at 20 knots at a heading of 45 degrees with a reference velocity error of one knot and a heading error of ten arc minutes results in an error in the estimation of the misalignment angle of less than one arc second, the resolution of this report's calibration technique.

The author now shows the computations performed to determine the "perturbation" velocity containing the misalignment angle information resulting from the periodic application of positive and negative torques to the vertical gyro. The resultant velocity of concern is the velocity which has been corrected for possible errors in the reference velocity. The Laplace Transform of this velocity is given by Equation A.7. The first term of Equation A.7 will only be analyzed in the following work. However, the second term was analyzed by the author in the same fashion and the result of that analysis has been presented in Equation A.8.

The "perturbation" acceleration input signal to the system was illustrated in Figure 4.3 of Chapter IV and is repeated here in Figure A.3. This periodic signal satisfies the conditions of the Fourier Series Theorem (Reference 15) which enables the author to represent the signal by a Fourier Series. In addition, the signal possesses odd quarter-wave symmetry and can be represented by the Fourier Series given by Equation A.9.

$$a(t) = \sum_{k=1}^{\infty} B_{2k-1} \sin(2k-1) \frac{2\pi}{T} t \quad (A.9)$$

where

$$B_{2k-1} = \frac{8}{T} \int_0^{T/4} a(t) \sin(2k-1) \frac{2\pi}{T} t dt \quad (A.10)$$

$$a(t) = -g \theta \sin \dot{\alpha} t \quad (\text{valid over } 0 < t < T/4) \quad (A.11)$$

$$T = 8 \text{ minutes (the perturbation period)}$$

$$\dot{\alpha} = 120 \text{ degrees per hour}$$

$$g = \text{gravitational acceleration}$$

Substituting Equation A.11 into A.10 and performing the integration

$$B_{2k-1} = \frac{8 g \theta \dot{\alpha} T (-1)^k \cos \dot{\alpha} T / 4}{4\pi^2 (2k-1)^2 - (\dot{\alpha} T)^2} \quad (A.12)$$

Inserting A.12 into A.9 and substituting the values for  $\dot{\alpha}$  and  $T$ , the Fourier Series for the acceleration signal becomes

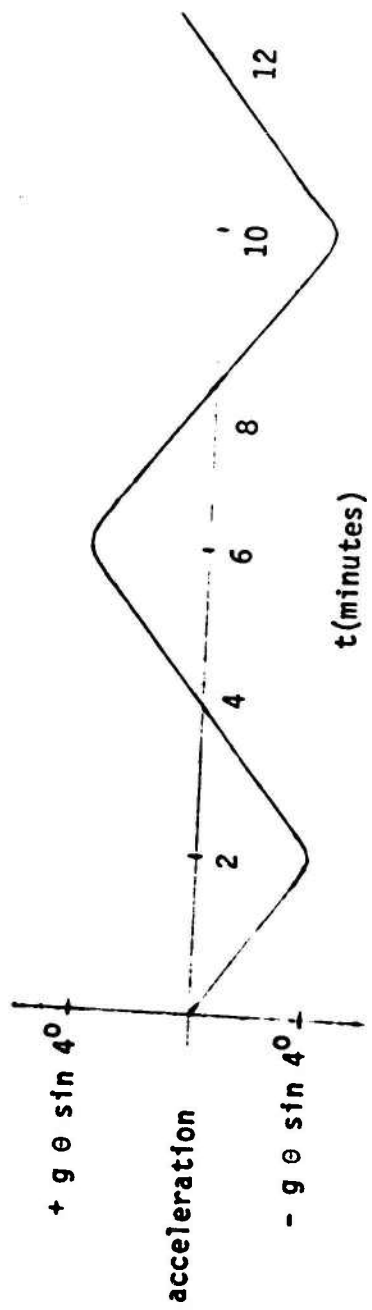
$$a(t) = 0.05645 g \theta \sum_{k=1}^{\infty} b_{2k-1} (-1)^k \sin(2k-1) \frac{2\pi}{T} t \quad (A.13)$$

where

$$b_{2k-1} = \frac{(45)^2}{(45(2k-1))^2 - 4} \quad (A.14)$$

Laplace transforming Equation A.13, we have

$$\mathcal{L}\{a(t)\} = \sum_{k=1}^{\infty} A_{2k-1} \frac{w_{2k-1}}{s^2 + w_{2k-1}^2} \quad (A.15)$$



ACCELERATION ERROR SIGNAL

FIGURE A.3

where

$$A_{2k-1} = 0.05645 g \theta b_{2k-1} (-1)^k$$

$$\omega_{2k-1} = + (2k-1) 15 \pi \text{ radians per hour}$$

The value for the resultant velocity is from Equation A.7

$$v_x(t) = \mathcal{L}^{-1} \left[ \sum_{k=1}^{\infty} \frac{s^2 + \sigma s}{s^3 + \sigma s^2 + s\omega_s^2 + \beta\omega_s^2} A_{2k-1} \cdot \frac{\omega_{2k-1}}{s^2 + \omega_{2k-1}^2} \right] \quad (\text{A.16})$$

Values for  $\sigma$  and  $\beta$  were calculated by the author to give the system a damping factor of 0.3.

$$\sigma = 3.5$$

$$\beta = 1.0$$

In the remaining analysis, the author uses the value of the gravitational acceleration,  $g$ , at a latitude equal to 45 degrees. At other latitudes, an excellent value for  $g$  can be obtained from the International Gravity Formula given by Equation A.17.

$$g (\text{ft./sec}^2) = 32.087664 + 0.170141 \sin^2 L - 0.0001877 \sin^2 2L \quad (\text{A.17})$$

The value for the Schuler Frequency at latitude of 45 degrees is

$$\omega_s = \sqrt{g/R} = 4.4667 \text{ radians per hour}$$

where  $R$  equals the earth's radius at a latitude of 45 degrees.

Performing the calculations and the inverse Laplace Transformation required by Equation A.16 and summing over the first 15 values gives the value for the resulting velocity accurate to the number of digits displayed in Equation A.18 and Equation A.19.

$$v_x(t) = -83.043 \theta \cos(\omega_\theta t) + f(t) \quad (\text{A.18})$$

where

$$f(t) = \begin{aligned} & 13.617 \theta \exp(-1.157 t) \\ & -95.937 \theta \exp(-1.171 t) \cos(3.9835 t - 14^\circ) \\ & - \theta \sum_{k=2}^{\infty} Z_{2k-1} \cos((2k-1)W_\theta t) \end{aligned} \quad (A.19)$$

and where

$$W_\theta = 15 \pi \text{ rad/hr} \text{ (the perturbation frequency)}$$

$$Z_{2k-1} = \text{amplitudes of the frequencies } (2k-1) W_\theta$$

Equation A.18 is the Chapter IV equation used in formulating the method for the estimation of the misalignment angle,  $\theta$ . Equation A.19 is composed of the secondary effects referred to in Chapter IV. The third term of Equation A.19 represents the velocity resulting from the higher frequencies of the Fourier Series used to describe the input acceleration signal. These higher frequency terms, besides being small compared to the perturbation frequency term of Equation A.18, are attenuated by the velocity averaging process described in Chapter IV. The averaging occurs  $\pm 12$  seconds from a peak value of these signals. After the completion of the averaging process and the employment of the estimation equation of Chapter IV, the resulting contribution to the estimation of the misalignment angle is  $-2.477 K \theta$ . This term must be added to the pure perturbation frequency term of  $83.043 K \theta$  resulting in a value of  $80.566 K \theta$ . The value for  $K$ , the conversion factor, now becomes  $42.670 \text{ min/knot}$ .

The first and second terms of Equation A.19 are Schuler disturbance terms resulting from the calibration technique. These terms are slowly varying functions compared to the perturbation signal and are attenuated by the estimation procedure used by the author. Their effective error contributions to the estimation of the misalignment angle are  $0.44 K \theta$ ,  $0.008 K \theta$ ,  $-0.173 K \theta$  and  $0.002 K \theta$  for the first four estimation terms (assuming the calibration procedure is continued beyond the time (25

minutes) for the first estimate). The maximum error contribution is 0.55% of the true misalignment angle and therefore can be neglected.

## APPENDIX B

This appendix presents the calculations performed to obtain the equation for the estimator of the misalignment angle using the method of least squares. The appendix also provides the calculations, under certain assumptions, for obtaining the confidence limits for the misalignment angle. Finally, the appendix delineates the procedure to obtain more efficient estimators of the misalignment angle.

### Misalignment Angle Estimator

The generalized model for the resultant velocity is presented in Equation A.1 wherein the misalignment angle is obtained by multiplying the term, B, by the conversion factor K, that is ( $\theta = KB$ ). The parameters B,  $B_0$  and  $B_1$  are assumed to be constant over the time of estimation. The term  $e_i$  is a random variable representing the random noise error in the observations and  $V_i$  represents the  $i^{\text{th}}$  observed velocity data.

$$V_i = (-1)^{i+1} B + B_0 + B_1 t_i + e_i \quad (\text{A.1})$$

where  $i = 1, 2, \dots, n$

According to the method of least squares we form the sum of the error terms squared, Equation A.2, and choose our estimates  $b$ ,  $b_0$  and  $b_1$  to be the values which, when substituted for B,  $B_0$  and  $B_1$  in Equation A.2, minimize the value S.

$$S = \sum_{i=1}^n e_i^2 = \sum_{i=1}^n (V_i - (-1)^{i+1} B - B_0 - B_1 t_i)^2 \quad (\text{A.2})$$

We determine  $b$ ,  $b_0$  and  $b_1$  by differentiating Equation A.2 with respect to the parameters B,  $B_0$  and  $B_1$  and setting the results equal to zero. We obtain

$$\begin{aligned}\frac{\partial S}{\partial B} &= -2 \left( \sum_{i=1}^n (-1)^{i+1} (v_i - (-1)^{i+1} B - B_0 - B_1 t_i) \right) = 0 \\ \frac{\partial S}{\partial B_0} &= -2 \left( \sum_{i=1}^n (v_i - (-1)^{i+1} B - B_0 - B_1 t_i) \right) = 0 \\ \frac{\partial S}{\partial B_1} &= -2 \left( \sum_{i=1}^n t_i (v_i - (-1)^{i+1} B - B_0 - B_1 t_i) \right) = 0\end{aligned}\quad (\text{A.3})$$

so that the estimates  $b$ ,  $b_0$  and  $b_1$  are given by

$$\begin{aligned}\sum_{i=1}^n (-1)^{i+1} (v_i - (-1)^{i+1} B - B_0 - B_1 t_i) &= 0 \\ \sum_{i=1}^n (v_i - (-1)^{i+1} B - B_0 - B_1 t_i) &= 0 \\ \sum_{i=1}^n t_i (v_i - (-1)^{i+1} B - B_0 - B_1 t_i) &= 0\end{aligned}\quad (\text{A.4})$$

where we substitute  $(b, b_0, b_1)$  for  $(B, B_0, B_1)$  when we equate Equation A.4 to zero. From Equation A.4 we obtain

$$\begin{aligned}nb + b_0 \sum_{i=1}^n (-1)^{i+1} + b_1 \sum_{i=1}^n (-1)^{i+1} t_i &= \sum_{i=1}^n (-1)^{i+1} v_i \\ b \sum_{i=1}^n (-1)^{i+1} + nb_0 + b_1 \sum_{i=1}^n t_i &= \sum_{i=1}^n v_i \\ b \sum_{i=1}^n (-1)^{i+1} t_i + b_0 \sum_{i=1}^n t_i + b_1 \sum_{i=1}^n t_i^2 &= \sum_{i=1}^n t_i v_i\end{aligned}\quad (\text{A.5})$$

The solution of Equation A.5 for  $b$  is

$$b = \frac{AX - CY}{DA + C^2} \quad (\text{A.6})$$

where

$$A = \left( \sum_{i=1}^n t_i^2 \right) - n \sum_{i=1}^n t_i^2$$

$$X = n \sum_{i=1}^n (-1)^{i+1} v_i - \sum_{i=1}^n (-1)^{i+1} \sum_{j=1}^n v_j$$

$$C = n \sum_{i=1}^n (-1)^{i+1} t_i - \sum_{i=1}^n (-1)^{i+1} \sum_{j=1}^n t_j$$

$$Y = \sum_{i=1}^n t_i \sum_{i=1}^n v_i - n \sum_{i=1}^n t_i v_i$$

$$D = n^2 - \left( \sum_{i=1}^n (-1)^{i+1} \right)^2$$

From the restrictions placed on the model of observing six data values, one every four minutes

$$n = 6$$

$$t_i = 0, 4, 8, 12, 16, 20 \quad i = 1, 2, 3, 4, 5, 6$$

Substituting these values into Equation A.6 we obtain

$$b = 1/48 (5v_1 - 11v_2 + 8v_3 - 8v_4 + 11v_5 - 5v_6) \quad (\text{A.7})$$

Multiplying by the conversion factor, K, we obtain for the misalignment angle,  $\theta$ , the estimator

$$\hat{\theta} = K/48 (5v_1 - 11v_2 + 8v_3 - 8v_4 + 11v_5 - 5v_6). \quad (\text{A.8})$$

#### Misalignment Angle Confidence Limits

To obtain the confidence limits for the misalignment angle, it is assumed that the error term is independently and normally distributed with mean zero and variance  $\sigma^2$ , and that the model is a correct representation of the observed velocity data. Under these assumptions  $s_R^2$  given by Equation A.9 is an estimate of  $\sigma^2$  (Reference (14)).

$$s_R^2 = 1/3 \sum_{i=1}^6 (v_i - (-1)^{i+1} b - b_0 - b_1 t_i)^2 \quad (\text{A.9})$$

We now find  $s_R^2$  in terms of the observed data values. The estimators  $b_0$  and  $b_1$  are obtained in the same fashion as  $b$  and are given by Equations A.10 and A.11 respectively.

$$b_0 = 1/48 (23(v_1+v_2) + 8(v_3+v_4) - 7(v_5+v_6)) \quad (\text{A.10})$$

$$b_1 = 3/9 (v_5+v_6-v_1-v_2) \quad (\text{A.11})$$

Substituting Equations A.7, A.10 and A.11 into A.9, we obtain

$$s_R^2 = 1/36 \begin{bmatrix} +5(v_1^2 + v_2^2 + v_5^2 + v_6^2) & -2(v_1v_5 + v_2v_6) \\ +8(v_3^2 + v_4^2 - v_1v_3 - v_2v_4 - v_3v_5 - v_4v_6) \\ -6(v_1v_2 + v_5v_6 - v_1v_6 - v_2v_5) \end{bmatrix} \quad (A.12)$$

In addition it can be shown, Reference (13), that the random variable  $3s_R^2/\sigma^2$  has a chi-square distribution with 3 degrees of freedom and that it is distributed independently of  $b$ ,  $b_0$ ,  $b_1$  and  $\hat{\theta}$ . Also, based on the previous assumptions,  $\hat{\theta}$  is independently normally distributed since by Equation A.8 it is formed from a linear combination of independent normal random variables, the  $v_i$ 's. Noting that

$$\begin{aligned} E(v_i) &= (-1)^{i+1} b + b_0 + b_1 t_i \\ \text{Var}(v_i) &= \sigma^2 \end{aligned} \quad (A.13)$$

we compute the expected value and variance of  $\hat{\theta}$  from Equation A.8 as

$$\begin{aligned} E(\hat{\theta}) &= K B = \theta \\ \text{Var}(\hat{\theta}) &= \sigma_{\hat{\theta}}^2 = 35/192 K^2 \sigma^2 \end{aligned} \quad (A.14)$$

and form a standardized normal variable (mean zero and standard deviation one)

$$\frac{\hat{\theta} - E(\hat{\theta})}{\sqrt{\text{Var}(\hat{\theta})}} = \frac{\hat{\theta} - \theta}{K \sqrt{35/192}} \quad (A.15)$$

We now derive the expression for the confidence limits from the basic definition of the student-t distribution; i.e., the ratio of two independent random variables, the numerator being normal with mean zero and standard deviation one and the denominator being the square root of a chi-square random variable divided by its degrees of freedom. We have, using the previously determined chi-square and standardized normal random variables,

$$t(3 \text{ deg. of freedom}) = \frac{\hat{\theta} - \theta}{\frac{K\sqrt{35/192}}{\sigma^2}} \div \sqrt{\frac{3s_R^2}{\sigma^2}}$$

$$= \frac{\hat{\theta} - \theta}{s_{\theta}} \quad (\text{A.16})$$

where  $s_{\theta}$  is the estimated standard deviation of  $\hat{\theta}$  and is given by

$$s_{\theta} = Ks_R \sqrt{35/192} \quad (\text{A.17})$$

From a student-t distribution, we have

$$\Pr \left[ -t(3, (1-\alpha/2)) \leq t \leq t(3, (1-\alpha/2)) \right] = 1-\alpha \quad (\text{A.18})$$

where  $t(3, 1-\alpha/2)$  is the  $(1-\alpha/2)$  percentage point of the student-t distribution with 3 degrees of freedom. Substituting Equation A.16 into A.18

$$\Pr \left[ -t(3, (1-\alpha/2)) \leq \frac{\hat{\theta} - \theta}{s_{\theta}} \leq t(3, (1-\alpha/2)) \right] = 1-\alpha \quad (\text{A.19})$$

or

$$\Pr \left[ \hat{\theta} - t(3, (1-\alpha/2))s_{\theta} \leq \theta \leq \hat{\theta} + t(3, (1-\alpha/2))s_{\theta} \right] = 1-\alpha \quad (\text{A.20})$$

Thus the  $(1-\alpha/2)$  confidence limits for  $\theta$  are

$$\theta = \hat{\theta} \pm t(3, 1-\alpha/2)s_{\theta} \quad (\text{A.21})$$

### More Efficient Misalignment Angle Estimators

To obtain more efficient estimators of the misalignment angle, we note from the previous assumptions that  $\hat{\theta}$  is independently normally distributed. Having  $n$  samples of  $\hat{\theta}$ , the best unbiased estimator of  $\theta$  is (Reference (3))

$$\hat{\bar{\theta}} = 1/n \sum_{i=1}^n \hat{\theta}_i \quad (\text{A.22})$$

where  $\hat{\bar{\theta}}$  has a mean and variance

$$E(\hat{\theta}) = \theta$$

$$\text{Var}(\hat{\theta}) = \sigma_{\theta}^2/n = (35/192)K^2 \sigma^2/n \quad (\text{A.23})$$

To obtain the new confidence limits for  $\theta$  based on the estimate given by Equation A.22, we proceed as follows: Having  $n$  independent samples of  $s_R^2$ , we form  $n$  independent chi-square random variables

$$3s_{R_i}^2 / \sigma^2 \quad i=1, 2, 3, \dots, n \quad (\text{A.24})$$

Using the reproductive property of the chi-square variate, the random variable

$$\sum_{i=1}^n \frac{3s_{R_i}^2}{\sigma^2}$$

formed from Equation A.24 has a chi-square distribution with  $3n$  degrees of freedom and is distributed independently of  $\hat{\theta}$ . From the basic definition of the student-t distribution

$$t_{3n} = \frac{\hat{\theta} - \theta}{\sigma_{\theta} / \sqrt{n}} \pm \sqrt{\sum_{i=1}^n \frac{3s_{R_i}^2 / \sigma^2}{3n}} \quad (\text{A.25})$$

$$= \frac{\hat{\theta} - \theta}{(1/n)\sqrt{35/192} K \sqrt{\sum_{i=1}^n s_{R_i}^2}}$$

From Equation A.17

$$s_{\theta_i} = K s_{R_i} \sqrt{35/192} \quad (\text{A.26})$$

or

$$\sqrt{\sum_{i=1}^n s_{\theta_i}^2} = \sqrt{35/192} K \sqrt{\sum_{i=1}^n s_{R_i}^2}$$

Thus

$$t_{3n} = \frac{\hat{\theta} - \theta}{(1/n)\sqrt{\sum_{i=1}^n s_{\theta_i}^2}} \quad (\text{A.27})$$

Letting

$$\bar{s}_\theta = (1/n) \sqrt{\sum_{i=1}^n s_{\theta_i}^2} \quad (\text{A.28})$$

and following the same procedure as outlined by Equations A.18 through A.21, the  $(1-\alpha)$  confidence limits for  $\theta$  now become

$$\theta = \hat{\theta} \pm t(3n, 1-\alpha/2) \bar{s}_\theta \quad (\text{A.29})$$